Life Sciences 232 (2019) 116681

Contents lists available at ScienceDirect

Life Sciences

journal homepage: www.elsevier.com/locate/lifescie

Perturbed ovarian and uterine glucocorticoid receptor signaling accompanies the balanced regulation of mitochondrial function and NFκB-mediated inflammation under conditions of hyperandrogenism and insulin resistance

Min Hu[a,b], Yuehui Zhang[b,c], Xiaozhu Guo[c], Wenyan Jia[c], Guoqi Liu[c], Jiao Zhang[d], Peng Cui[b,e], Juan Li[a,b], Wei Li[c], Xiaoke Wu[c], Hongxia Ma[a], Mats Brännström[f], Linus R. Shao[b,*], Håkan Billig[b]

[a] Department of Traditional Chinese Medicine, The First Affiliated Hospital of Guangzhou Medical University, 510120 Guangzhou, China
[b] Department of Physiology/Endocrinology, Institute of Neuroscience and Physiology, The Sahlgrenska Academy, University of Gothenburg, 40530 Gothenburg, Sweden
[c] Department of Obstetrics and Gynecology, Key Laboratory and Unit of Infertility in Chinese Medicine, First Affiliated Hospital, Heilongjiang University of Chinese Medicine, 150040 Harbin, China
[d] Department of Acupuncture and Moxibustion, Second Affiliated Hospital, Heilongjiang University of Chinese Medicine, 150040 Harbin, China
[e] Department of Obstetrics and Gynecology, Shuguang Hospital Affiliated to Shanghai University of Traditional Chinese Medicine, 201203 Shanghai, China
[f] Department of Obstetrics and Gynecology, Sahlgrenska University Hospital, Sahlgrenska Academy, University of Gothenburg, 41345 Gothenburg, Sweden

ARTICLE INFO

Keywords:
Glucocorticoid receptor
11HSD
Mitochondrial malfunction
NFκB
Inflammation
Ovary
Uterus
Polycystic ovary syndrome

ABSTRACT

Aim: This study aimed to determine whether glucocorticoid receptor (GR) signaling, mitochondrial function, and local inflammation in the ovary and uterus are intrinsically different in rats with hyperandrogenism and insulin resistance compared to controls.

Main methods: Female Sprague Dawley rats were exposed to daily injections of human chorionic gonadotropin and/or insulin.

Key findings: In both the ovary and the uterus, decreased expression of the two GR isoforms was concurrent with increased expression of *Fkbp51* but not *Fkbp52* mRNA in hCG + insulin-treated rats. However, these rats exhibited contrasting regulation of *Hsd11b1* and *Hsd11b2* mRNAs in the two tissues. Further, the expression of several oxidative phosphorylation-related proteins decreased in the ovary and uterus following hCG and insulin stimulation, in contrast to increased expression of many genes involved in mitochondrial function and homeostasis. Additionally, hCG + insulin-treated rats showed increased expression of ovarian and uterine NFκB signaling proteins and *Tnfaip3* mRNA. The mRNA expression of *Il1b*, *Il6*, and *Mmp2* was decreased in both tissues, while the mRNA expression of *Tnfa*, *Ccl2*, *Ccl5*, and *Mmp3* was increased in the uterus. Ovaries and uteri from animals co-treated with hCG and insulin showed increased collagen deposition compared to controls.

Significance: Our observations suggest that hyperandrogenism and insulin resistance disrupt ovarian and uterine GR activation and trigger compensatory or adaptive effects for mitochondrial homeostasis, allowing tissue-level maintenance of mitochondrial function in order to limit ovarian and uterine dysfunction. Our study also suggests that hyperandrogenism and insulin resistance activate NFκB signaling resulting in aberrant regulation of inflammation-related gene expression.

1. Introduction

Worldwide, 4%–21% of all adolescent and reproductive-aged women are diagnosed with polycystic ovary syndrome (PCOS), which is a complex, heterogeneous hormone-imbalance disorder [1]. Extensive evidence from clinical studies suggests that PCOS patients commonly have impaired ovarian folliculogenesis and chronic anovulation. Additionally, their endometrium tends to remain in a proliferative state [2], which might result in disrupted processes of uterine decidualization and embryo implantation [3,4]. These defects cause approximately 75% of PCOS patients to suffer from anovulation infertility [5], and approximately 50% of PCOS patients experience recurrent pregnancy loss [6]. Although hyperandrogenism and insulin resistance either alone or in combination are recognized as the central manifestations in

* Corresponding author.
E-mail address: linus.r.shao@fysiologi.gu.se (L.R. Shao).

https://doi.org/10.1016/j.lfs.2019.116681
Received 2 May 2019; Received in revised form 16 July 2019; Accepted 21 July 2019
Available online 23 July 2019
0024-3205/

PCOS patients [7–9], the precise pathophysiological mechanisms of this syndrome that result in disrupted ovarian and uterine function are far from completely understood.

Glucocorticoid receptor (GR) is a ligand-dependent transcription-regulating protein belonging to the steroid receptors within the superfamily of nuclear receptors [10]. Among its other functions [10], GR plays a critical role in female reproduction [11]. Specifically, GR is highly expressed in the mammalian ovary and uterus [12,13], and genetic models have demonstrated a physiological role for GR as a required factor in embryo implantation and decidualization [14]. The GRα and GRβ isoforms are encoded in both humans and rodents, and there is compelling evidence that cellular GRα, but not GRβ, is principally activated by ligand-binding such as cortisol in humans and corticosterone in rodents [10,11]. Human studies have previously reported that the use of dexamethasone, an exogenous glucocorticoid drug, induces abnormal glucose homeostasis and impairs peripheral insulin sensitivity [15,16]. Similarly, treatment with dexamethasone results in peripheral and tissue-specific insulin resistance and decreased ovarian 17β-estradiol production in different animal models [17–19]. While systemic and tissue-specific insulin resistance is often seen in PCOS patients [8,9] and PCOS-like animal models [20–22], intracellular GR signaling might be maintained and continue to play a critical role in PCOS. Supporting this notion, clinical studies have demonstrated a positive correlation between elevated local cortisol levels and ovarian and endometrial insulin resistance in PCOS patients [23,24]. In addition to insulin resistance, hyperandrogenism, particularly of ovarian origin, is the cornerstone of PCOS pathophysiology [7], and several studies have reported the aberrant expression of ovarian and endometrial androgen receptor (AR) in PCOS patients compared to non-PCOS controls [25–27]. Because there is high similarity in the DNA-binding domains, the ligand-binding domains, and the hormone-response elements between GR and AR [28], it would be most informative to study the molecular mechanisms of ovarian and uterine GR signaling under the conditions of hyperandrogenism and/or insulin resistance *in vivo*.

It is notable that some [29,30], but not all, clinical studies have shown that elevated circulating cortisol levels and its metabolism are associated with PCOS [31]. However, increased expression and activity of intracellular 11β-hydroxysteroid dehydrogenase (11βHSD) 1, the pre-receptor regulator of glucocorticoids, determines the local cortisol concentrations in a tissue-specific manner [32], as reported in adipose tissues of PCOS patients [33]. 11βHSD, which is a member of the short-chain dehydrogenase/reductase superfamily, is important for intracellular glucocorticoid metabolism and action in the target tissues/cells [34]. It is expressed as two isoforms, 11βHSD1 (*Hsd11b1*) and 11βHSD2 (*Hsd11b2*), and they are co-expressed in most tissues, including the ovary and uterus in both humans and rodents [11,34]. In humans, while 11βHSD1 functions mainly as a reductase converting inactive cortisone to active cortisol, 11βHSD2 acts exclusively as an oxidase converting cortisol to cortisone [34]. In rodents, corticosterone is a main active glucocorticoid, whereas 11-dehydrocorticosterone is an inactive glucocorticoid [34]. The functional roles of 11βHSD1 and 11βHSD2 in rodents are similar to those in humans. These findings suggest that the distinct expression patterns and enzymatic activities of 11βHSD isoforms might change in opposite directions in order to regulate the local concentration of cortisol/corticosterone in a particular tissue or cell type. In addition, the tissue-specific regulation of the 11βHSD isoforms in response to a variety of pathophysiological stimuli has been investigated as a potential method for activating or suppressing the GR signaling pathway [32,34]. However, the causality of 11βHSD isoform dysregulation in the ovary and uterus under the conditions of hyperandrogenism and/or insulin resistance has never to our knowledge been experimentally determined in a PCOS-like animal model *in vivo*.

In addition to the nuclear translocation of GR from the cytoplasm [10,11], it can also be translocated to the mitochondria in many different cell types [35]. While mitochondria play a dynamic and multifaceted role in cell signaling and metabolism [36], several studies have demonstrated that mitochondrial GR contributes to the regulation of mitochondrial DNA gene transcriptional responses in a similar manner as it functions in the nucleus [35]. In fact, *in vivo* and *in vitro* studies have demonstrated that mitochondrial DNA (mtDNA) contains glucocorticoid response elements that can regulate mtDNA transcription in a ligand-dependent manner [37,38]. In PCOS patients and PCOS-like animals, there is evidence that hyperandrogenism and insulin resistance impair mitochondrial function in different tissues and cells *in vivo* [26,39–45]. In addition, while glucocorticoid-mediated regulation of inflammatory and immune responses as well as female fertility is well studied [10,11], clinical studies also show a strong and frequent correlation between the development of PCOS and low-grade chronic inflammation [1,3,4]. Work by our group and others indicates that adult rats treated chronically with human chorionic gonadotropin (hCG) and insulin display several features of PCOS such as follicular cyst formation [22], ovarian and uterine insulin resistance, and changes in glucose metabolism [20,46,47] in addition to hyperandrogenism and metabolic dysfunction [20,22,41,46,48–51]. However, the cellular significance of the connection between hyperandrogenism and insulin resistance and glucocorticoid-GR signaling-mediated mitochondrial function and chronic inflammation in the ovary and uterus remains unclear.

In the present study, we comprehensively examined the distribution and alteration of GR signaling, mitochondrial function, and local inflammation in the rat ovary and uterus in response to chronic treatment with hCG and/or insulin, which mimic two of the main PCOS-related etiological factors. Our findings indicate that aberrant changes in GR expression and functionality might be involved in the pathological ovarian and uterine processes in PCOS patients.

2. Materials and methods

2.1. Ethics approval and animal care

All animal experiments and animal care procedures were carried out according to the institutional guidelines for the care and use of animals in research. The studies were approved by the Animal Care and Use Committee of the Heilongjiang University of Chinese Medicine, China (HUCM 2015-0112).

Adult female Sprague Dawley rats (70 days old) were obtained from the Laboratory Animal Centre of Harbin Medical University (Harbin, China) and were kept in groups with free access to food and water and a controlled temperature of 22 ± 2 °C with a 12:12 h light:dark cycle.

2.2. Chemicals and reagents

hCG was from NV Organon (Oss, Holland), and human recombinant insulin (Humulin NPH) was from Eli Lilly Pharmaceuticals (Giza, Egypt). Anti-mouse IgG horseradish peroxidase (HRP)-conjugated goat (A2304), and anti-rabbit IgG HRP-conjugated goat (A0545) secondary antibodies were from Sigma-Aldrich (St. Louis, MO). The primary antibodies used for Western blot and immunohistochemical analyses in the present study, their dilutions, and their sources are listed in Table 1. The avidin-biotinylated-peroxidase complex detection system (ABC kit) was from Vector Laboratories Inc. (Burlingame, CA). A detailed list of primers is provided in Table 2. Unless otherwise specified, all reagents were purchased from Sigma-Aldrich (St Louis, MO, USA).

2.3. Study design, estrous cycle analysis, and tissue collection

The female Sprague Dawley rats (n = 98) used in this study needed to have normal cycles prior to treatment, and these were confirmed by examination of vaginal smears under a light microscope for two sequential estrous cycles (about 8–10 days). All rats were randomly divided into four groups and treated with (A) an equal volume of saline as

Table 1
The species, catalog number, method, dilution and source of antibodies.

Antibody	Species	Code	kDa	Method	Dilution	Source
GR	Rabbit	3660	94/91	WB IHC	1:1000 1:100	Cell Signaling Technology (Danver, MA)
Total OXPHOS	Mouse	110,413	I 20 II 30 III 48 IV 40 V 55	WB	1:500	Abcam (Cambridge, UK)
IKKβ	Rabbit	8943	87	WB	1:1000	Cell Signaling Technology
IκBα	Mouse	4814	39	WB	1:1000	Cell Signaling Technology
p-NF-κB p65	Rabbit	3033	65	WB	1:500	Cell Signaling Technology
NF-κB p65	Rabbit	8242	65	WB	1:1000	Cell Signaling Technology

GR, glucocorticoid receptor; Total OXPHOS, total oxidative phosphorylation; IKKβ, IkappaB kinase β; IκBα, nuclear factor of kappa light polypeptide gene enhancer in B-cells inhibitor alpha; p-NF-κB, phosphorylation of nuclear factor kappa-light-chain-enhancer of activated B cells; WB, Western blot analysis; IHC, immunohistochemistry.

controls, (B) 3.0 IU/day hCG to induce hyperandrogenism, (C) insulin, which was started at 0.5 IU/day and gradually increased to 6.0 IU/day between the 1st day and the 10th day and was then given at 6.0 IU/day until the 22nd day to induce hyperinsulinemia and peripheral insulin resistance, or (D) hCG plus insulin to induce a combination of hyperandrogenism and peripheral insulin resistance, which are key copathologies of PCOS. All animals were exposed to saline, hCG, and/or insulin for 22 days and decapitated on the 23rd day of treatment. The doses and treatment protocols for hCG and insulin are described in detail in our previous paper [20].

Prior to treatment, estrous cycles were monitored daily by vaginal lavage according to a standard protocol [52]. Rats treated with saline or insulin had normal cycles, but hCG-treated and hCG + insulin-treated animals displayed absent or prolonged cycles. None of the hCG + insulin-treated rats with prolonged estrous cycles were included in the study. After treatment, 10 animals per group were randomly selected and further analyzed.

After transient anesthesia by isoflurane (2% in a 1:1 mixture of oxygen or air, RWD Life Science Co., Shenzhen, China), the ovaries and uteri were removed and stripped of fat and connective tissues. One side of the ovary and uterus in each animal was fixed in 4% formaldehyde and neutral buffered solution for 24 h at 4 °C and embedded in paraffin for histochemical analysis. The other side was immediately frozen in liquid nitrogen and stored at −70 °C for subsequent quantitative real-time (qRT) PCR and Western blot analyses.

2.4. Morphological assessment, immunostaining, and imaging

Whole mount images were taken of freshly dissected ovaries and uteri after decapitation. The fixed tissues, including the ovaries and uteri, were embedded in paraffin. Sections were cut at a thickness of 5 μm and stained with hematoxylin and eosin (H&E) according to standard procedures, and the immunohistochemical staining was performed as previously described [48,49]. Ovarian and uterine tissue sections were dewaxed and refixed in Bouin's solution (HT10132, Sigma-Aldrich) and stained with Weigert's Iron Hematoxylin Set (HT10-79, Sigma-Aldrich) and Masson's Trichrome Staining Kit (HT15, Sigma-Aldrich) as described by the manufacturer. After deparaffinization and rehydration, the sections were immersed in epitope retrieval buffer (1 mM EDTA, 0.05% Tween 20, pH 8.0) and heated in a 700 W microwave for 15 min. The sections were subsequently rinsed twice with dH_2O and once with 0.01 M Tris-buffered saline supplemented with Triton X-100 (TBST). The endogenous peroxidase was removed, and nonspecific binding was blocked by incubation with 3% H_2O_2 for 10 min and then with 10% normal goat serum for 1 h at room temperature. After incubation with the anti-GR primary antibody (1:100 dilution, Table 1) overnight at 4 °C in a humidified chamber, sections were stained using the avidin-biotinylated-peroxidase ABC kit according to the manufacture's instructions (Vector Laboratories) followed by a 5-min treatment with 3,3-diaminobenzidine tetrahydrochloride (DAB, SK-4100, Vector Laboratories). All sections were incubated with DAB for the same length of time so that comparisons could be made between individual samples, and all slides were stained in a single run to eliminate inter-experiment variations in staining intensity. Tissue sections were observed with a Nikon E-1000 microscope (Japan) under bright-field optics and photomicrographed using Easy Image 1 (Bergström Instrument AB, Sweden).

2.5. DNA and RNA isolation, cDNA synthesis, and qRT-PCR analysis

The procedure to quantify mitochondrial/nuclear DNA was performed as previously described [40]. The details of ovarian and uterine RNA isolation, quantification, and quality assessment were described previously [20,40]. Each cDNA sample was subjected to qRT-PCR with a Roche Light Cycler 480 sequence detection system (Roche Diagnostics Ltd., Rotkreuz, Switzerland) using SYBR green qPCR master mix (K0252, Thermo Scientific, Rockford, IL). The mtDNA copy number was determined by measuring the DNA levels of *Nd4* and *Cytb* (mitochondrial genes) and *Actb* (a nuclear gene) by qRT-PCR. The primer sequences for each target gene are listed in Table 2. Several housekeeping genes, including *Gapdh*, *Actb*, and *U87*, were tested prior to analysis. *Gapdh* was chosen as the internal reference for all analyses because expression remained stable across all groups. Each sample was analyzed in triplicate, and the relative fold expression of each gene was calculated using the comparative critical threshold (Ct) method (Life Technologies, Stockholm, Sweden) with normalization to the *Gapdh* gene based on the $2^{-\Delta\Delta Ct}$ calculation.

2.6. Tissue protein extraction and Western blot analysis

Ovarian and uterine samples were pulverized and then homogenized in ice-cold RIPA buffer (Sigma-Aldrich) supplemented with cOmplete Mini protease inhibitor cocktail tablets (Roche Diagnostics, Mannheim, Germany) and PhosSTOP phosphatase inhibitor cocktail tablets (Roche Diagnostics). The protein extractions for whole cells and mitochondrial fractions were performed following published methodology [20,49,53]. After determining the total protein concentration by BCA assay, 30 μg of protein from each group was resolved on 4–20% TGX stain-free gels (Bio-Rad Laboratories GmbH, Munich, Germany) and transferred onto PVDF membranes. The membranes were blocked by 0.01 M Tris-buffered saline supplemented with Triton X-100 containing 5% nonfat dry milk for 1 h and were probed with different primary antibodies (Table 1) in the blocking buffer overnight at 4 °C followed by HRP-conjugated secondary antibody. Chemiluminiscence signals were detected using SuperSignal West Dura substrate following the manufacturer's instructions (Thermo Scientific—Pierce). Ultraviolet

Table 2
Primer sequences used for qRT-PCR measurement.

Gene	Primer Sequence (5′-3′)		Product size (bp)
Fkbp51 (*Fkbp5*)	Forward	TTTTGGAGAAGCGGGGAAAC	174
	Reverse	CCTCCCTTGAAGTACACCGT	
Fkbp52 (*Fkbp4*)	Forward	GCTGCCATCGAAAGCTGTAA	102
	Reverse	GTCAAAGTCATTCACGGCCA	
Hsd11b1	Forward	GTGGACTGGACATGCTCATTC	212
	Reverse	AGCAATCAGAGGTTGGGTCA	
Hsd11b2	Forward	CTGGCCACTGTGTTGGATTTG	122
	Reverse	TCCAGAACACGGCTGATATCCT	
Mfn1	Forward	GGAGATACAGGGCTACAGAAAC	104
	Reverse	AGCTCTTGCCACTACTTGTC	
Opa1	Forward	GTGTCAACGCATGTGATCGA	295
	Reverse	GGATGACCCTCAAGCTGTCT	
Drp1	Forward	GTGAGCCCGTGGATGATAAA	132
	Reverse	AAATCCTAGCACCACCACATAG	
Tfam	Forward	ACAAAGAAGCTGTGAGCAAGTA	99
	Reverse	GTGCTTTCTTCTTTAGGCGTTTC	
Pgc1a	Forward	GTGGATGAAGACGGATTGCC	219
	Reverse	GGTGTGGTTTGCATGGTTCT	
Nrf1	Forward	GGAAACTCAGAGCCACATTAGA	109
	Reverse	GCGCCAAACACCTTAAAGAC	
Parkin	Forward	CTCAGACAAGGACACATCAGTAG	110
	Reverse	TACATTGGAAGACCAAGACAGG	
Pink1	Forward	CAATGCCGCTGTGTATGAAG	108
	Reverse	GCTCCCTTTGAGACGACAT	
Rheb	Forward	ACGATCCAACCATAGAAAACACA	97
	Reverse	TATTCATCCTGCCCTGCTGT	
Atp13a	Forward	AGAGGGTCACTGCAAACAAC	98
	Reverse	GGTCCCTTCAATCCACACATAC	
Tnfa	Forward	ACCACGCTCTTCTGTCTACT	115
	Reverse	ATGATCTGAGTGTGAGGGTCT	
Tnfaip3	Forward	GGAGACAGACACTCGGAATTT	121
	Reverse	CAAGTTGTCCCATTCGTCATTC	
Il1b	Forward	ACCTGTCCTGTGTGATGAAAG	131
	Reverse	CTCCACTTTGGTCTTGACTTCT	
Il6	Forward	GCCTTCTTGGGACTGATGTT	95
	Reverse	GGTCTGTTGTGGGTGGTATC	
Ccl2	Forward	GATGCAGTTAATGCCCCACT	168
	Reverse	TTCCTTATTGGGGTCAGCAC	
Ccl5	Forward	CCAACCTTGCAGTCGTCTTT	75
	Reverse	CTTGAACCCACTTCTTCTCTGG	
Csf2	Forward	ACAGTTTCTCAGCACCCACC	109
	Reverse	TCCAGAGCACGCATGTCATT	
Mmp2	Forward	GCTGATACTGACACTGGTACTG	99
	Reverse	GATCTGAGCAATGCCATCAAAG	
Mmp3	Forward	AGATGCTGGCATGGAGGTTC	114
	Reverse	AAGGTACTGAAGCCACCGAC	
Nd4	Forward	AACTCAATAGGAACACTCAACTT	137
	Reverse	AGATGGACTCCGTATAATGGTA	
Cytb	Forward	GCAGCTTAACATTCCGCCCAATCA	92
	Reverse	TACTGGTTGGCCTCCGATTCATGT	
Actb	Forward	ATCATGTTTGAGACCTTCAACACCC	318
	Reverse	CATCTCTTGCTCGAAGTCTAGG	
Gapdh	Forward	TCTCTGCTCCTCCCTGTTCTA	121
	Reverse	GGTAACCAGGCGTCCGATAC	

Fkbp51 (*Fkbp5*), FK506 binding protein 5; *Hsd11b*, 11β-hydroxysteroid dehydrogenase; *Mfn1*, mitofusin 1; *Opa1*, optic atrophy 1, a dynamin-like GTPase; *Drp1*, dynamin related protein 1; *Tfam*, mitochondrial transcription factor A; *Pgc1a*, peroxisome proliferative activated receptor gamma coactivator 1 alpha; *Nrf1*, nuclear respiratory factor 1; *Pink1*, PTEN-induced putative kinase 1; *Rheb*, Ras homolog mTORC1 binding; *Atp13a*, ATPase cation transporting 13A2; *Tnfa*, tumor necrosis factor alpha; *Tnfaip3*, tumor necrosis factor alpha induced protein 3; *Il1b*, interleukin 1 beta; *Ccl2*, C-C motif chemokine ligand 2; *Csf2*, colony stimulating factor 2; *Mmp2*, matrix metallopeptidase 2; *Nd4*, NADH dehydrogenase subunit 4; *Cytb*, cytochrome *b*; *Actb*, actin beta; *Gapdh*, glyceraldehyde-3-phosphate dehydrogenase.

activation of the Criterion stain-free gel on a ChemiDoc MP Imaging System (Bio-Rad) was used to control for proper loading. Band densitometry and quantification was performed using Image Laboratory (Version 5.0, Bio-Rad, Sweden), and the protein band densities were normalized to the total-protein loading control. Details of the method have been described previously [48].

2.7. Transmission electron microscopy (TEM)

TEM was performed according to a published method [54]. Fresh ovarian and uterine tissues were excised and fixed in 2.5% glutaraldehyde in sodium phosphate (pH 7.2–7.4) for 1 min at room temperature (RT). After rinsing with 0.1 M phosphate-buffered saline (PBS, pH 7.2–7.4) three times for 15 min, the tissues were post-fixed with 1% osmium tetroxide in PBS for 1 h, followed by gradient dehydration in acetone (50%, 70%, and 90% for 15 min each and 100% three times for 30 min each time) at RT and then embedded in Epon epoxy resin. Random areas from the basal and labyrinth zones were oriented for ultrastructural analysis. Ultrathin sections were cut with a diamond knife using a Reichert ultramicrotome (Leica, Germany) at 50–60 nm thickness, collected on 300 mesh copper grids, and stained with 3% uranyl acetate and counterstained with lead citrate before visualization. Sections were examined and imaged with a transmission electron microscope (H-7650, Hitachi, Japan) equipped with an electron imaging spectrometer. Image collection and parameter settings were identical for each tissue analyzed.

2.8. Statistical analysis

For all experiments, n-values represent the numbers of individual animals. All values are presented as the means ± SEM. Statistical analyses were performed using the Statistical Package for Social Science (SPSS, version 24.0, SPSS Inc., Chicago, IL) and GraphPad Prism 5 statistical software (GraphPad Software, La Jolla, CA) for Windows. The normal distribution of the data was tested with the *Shapiro–Wilk test*. Differences between groups were analyzed by one-way ANOVA followed by *Tukey's post-hoc test* for normally distributed data or by the *Kruskal–Wallis test* for skewed data. Statistical significance was set at $p < 0.05$.

3. Results

3.1. Ovarian defects in rats treated chronically with hCG and/or insulin

In accordance with previous results from studies of follicular cyst formation and ovarian stromal hyperplasia in rodents treated with hCG and insulin [22,55], we found grossly oversized ovaries with enlarged fluid-filled follicles in hCG + insulin-treated and hCG-treated rats compared to control and insulin-treated rats (Fig. 1A). Further, morphological analysis revealed significant differences in the number of ovarian cystic follicles in hCG + insulin-treated and hCG-treated rats compared with the number in control and insulin-treated rats (Fig. 1A). In the ovaries, weak immunoreactivity was present in the cytoplasm of follicle cells (mainly in granulosa cells) and oocytes in control rats; however, there was intense nuclear GR immunoreactivity in the corpus luteum (Fig. 1B). In addition, GR immunoreactivity was almost completely absent in the apoptotic follicles in control rats (Fig. 1B). Because the GR consists of two distinct isoforms, GRα and GRβ [11], we performed a Western blot analysis to measure the expression of ovarian GR protein isoforms in rats treated chronically with hCG and/or insulin (Fig. 1C). There was no significant difference in GRα, GRβ, or total GR expression between saline-treated and insulin-treated rats. However, we observed that the expression of GRα and GRβ together with total GR was significantly decreased in hCG-treated rats compared to controls. Quantitative protein data indicated that GRα and total GR, but not GRβ, proteins were decreased in hCG + insulin-treated rats compared to control rats. Because FKBP5 (*Fkbp51*) and FKBP4 (*Fkbp52*), the GR binding proteins, display differential regulation of GR activation [56], we compared the expression of *Fkbp51* and *Fkbp52* mRNAs in the ovary by qRT-PCR (Fig. 1D). Quantitative data indicated that *Fkbp51* but not *Fkbp52* mRNA levels were increased in rats treated with hCG and/or

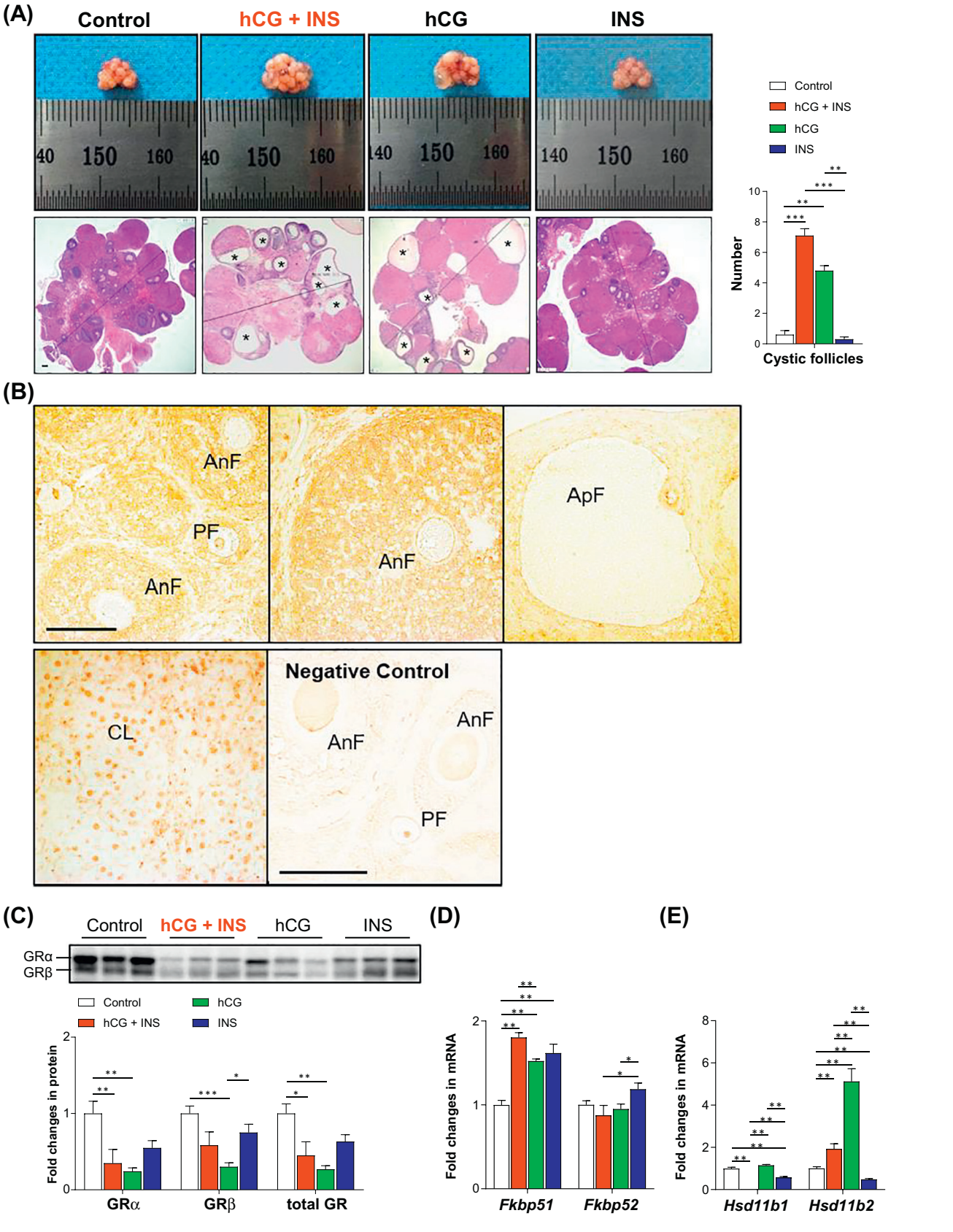

(caption on next page)

Fig. 1. Ovarian defects and impaired GR, *Fkbp5*, and *Hsd11b* expression in rats treated chronically with hCG and/or insulin. (A) Representative photographs of ovaries and images of H&E staining in the ovary and the effects of hCG and/or insulin on the number of ovarian cystic follicles. The stars indicate the ovarian cystic follicles. Scale bars (200 μm) are indicated in the photomicrographs. Values are means ± SEM (n = 10/group). **p < 0.01, ***p < 0.001. (B) Representative photomicrographs of immunohistochemical staining for ovarian GR in control rats. PF, primary follicle; AnF, antral follicle; CL, corpus luteum; ApF, apoptotic follicle. Scale bars (100 μm) are indicated in the photomicrographs. (C) Regulation of GR protein expression in the ovary. Protein levels were analyzed by Western blotting (n = 9/group). (D and E) Regulation of *Fkbp5* and *Hsd11b* gene expression in the ovary. mRNA levels were determined by qRT-PCR (n = 6/group). In all plots, data are presented as means ± SEM. *p < 0.05, **p < 0.01.

insulin compared to control rats treated with saline. This result suggests that Fkbp51, a negative regulator of GR activity, might be able to bind GR and block its activation in the ovary. While both 11βHSD1 (*Hsd11b1*) and 11βHSD2 (*Hsd11b2*) are expressed in the ovary [11,34], we found that the *Hsd11b1* mRNA level was decreased in hCG + insulin-treated and insulin-treated rats compared to controls. In contrast to insulin-treated rats, hCG + insulin-treated and hCG-treated rats exhibited an increase in *Hsd11b2* mRNA level (Fig. 1E).

GR function contributes not only to nuclear, but also to mitochondrial transcription [35]. To analyze whether the aberrant regulation of oxidative phosphorylation (OXPHOS) capacity – a key aspect of mitochondrial respiratory function [57] – is associated with decreased GR protein expression in the ovary after treatment with hCG and insulin, we profiled the expression of five respiratory protein complexes (Complex I, NADH dehydrogenase; Complex II, succinate dehydrogenase; Complex III, ubiquinol cytochrome *c* reductase; Complex IV, cytochrome *c* oxidase; and Complex V, ATP synthase) in the ovary. As shown in Fig. 2A, similar to GR protein regulation, the expression of OXPHOS Complex I, IV, and V was decreased in hCG + insulin-treated and hCG-treated rats compared to control rats. Among five respiratory protein complexes, only Complex II protein expression was increased in insulin-treated rats compared to control rats treated with saline. Next, we analyzed the gene expression profile, focusing on mitochondrial fusion (*Mfn1* and *Opa1*), fission (*Drp1*), biogenesis (*Tfam*, *Pgc1a*, and *Nrf1*), and mitophagy (*Parkin*, *Pink1*, *Rheb*, and *Atp13a*) [58]. As shown in Fig. 2B, although no significant difference was seen in *Mfn1*, *Tfam*, or *Pink1* mRNA expression between hCG + insulin-treated and control rats, increased expression of *Opa1*, *Drp1*, and *Pgc1a* mRNAs and decreased expression of *Nrf1*, *Parkin*, *Rheb*, and *Atp13a* mRNAs were found in hCG + insulin-treated rats. Additionally, there were similarities and differences in the gene expression patterns between hCG-treated and insulin-treated rats. For instance, we found increased expression of *Mfn1* and *Opa1* mRNAs and decreased *Atp13a* mRNA expression in hCG-treated and insulin-treated rats compared to controls. However, *Tfam* mRNA expression was decreased in hCG-treated rats but was increased in insulin-treated rats. Moreover, *Pink1* mRNA expression was unaltered in hCG-treated rats but was decreased in insulin-treated rats. Thus, the lack of significant effects of the combination of hCG and insulin on *Tfam* and *Pink1* mRNA expression is likely due to the contrasting effects of hCG and insulin. Similar to hCG + insulin-treated rats, decreased *Rheb* mRNA expression and increased *Drp1* and *Pgc1a* mRNA expression were found in hCG-treated and/or insulin-treated rats. The mtDNA copy number and mitochondrial morphology in the ovary were further analyzed by qRT-PCR and TEM. Although there was no difference in ovarian mtDNA copy number between control and different treatment groups (Fig. 3A), we observed that the mitochondria in the ovarian granulosa cells were significantly affected by hCG treatment alone and by co-treatment with hCG and insulin (Fig. 3B). For instance, mitochondria exhibited swelling, disrupted tubular cristae, blebbing, and decreased electron density. In addition, mitochondrial membrane rupture was observed in all treatment groups (Fig. 3B).

A dysfunctional or less sensitive GR promotes NFκB-mediated inflammatory processes [56,59]. Using Western blotting, we found that the expression of the inhibitor of NFkB kinase complex β (IKKβ) and nuclear factor of kappa light polypeptide gene enhancer in B-cells inhibitor alpha (IκBα) proteins was decreased in hCG + insulin-treated and hCG-treated rats (Fig. 4A). However, we found that while total NFκB (p65) protein expression was decreased, phosphorylated NFκB (p65) protein expression and the ratio of phosphorylated NFκB (p65) [p-NFκB (p65)] to total NFκB (p65) protein levels were significantly higher in hCG + insulin-treated rats compared to controls. While the pattern of total NFκB (p65) protein expression and the ratio of p-NFκB (p65) to total NFκB (p65) protein expression between hCG + insulin-treated and hCG-treated rats were similar, no alterations of any protein expression or the ratio of phosphorylated NFκB (p65) to total NFκB (p65) protein expression were found in insulin-treated rats (Fig. 4A). We next determined the expression pattern of genes that are involved in the inflammatory process in the ovary by qRT-PCR. Quantitative data indicated that *Tnfa*, *Il1b*, *Il6*, *Ccl2*, and *Csf2* mRNA expression was decreased by hCG and insulin treatment, both separately and in combination (Fig. 4B). Moreover, while *Tnfaip3* mRNA expression was increased in hCG + insulin-treated and insulin-treated rats, *Ccl5* mRNA expression was decreased in hCG + insulin-treated rats compared to control rats (Fig. 4B). Collagens are key structural protein components of the extracellular matrix [60], and altered matrix metalloproteinase (MMP) expression plays a role in the pathophysiology of the ovary and uterus [61]. In the ovary, we found that compared to control rats *Mmp2* mRNA expression was decreased in hCG + insulin-treated and hCG-treated rats and that *Mmp3* mRNA expression was decreased by hCG and insulin treatment, both separately and in combination (Fig. 4B). Furthermore, Masson's trichrome staining revealed that the deposition of ovarian collagen was significantly increased in hCG + insulin-treated rats compared to control rats (Fig. 4C). hCG-treated but not insulin-treated rats displayed similar ovarian collagen deposition as hCG + insulin-treated rats (data not shown).

3.2. Uterine defects in rats treated chronically with hCG and/or insulin

Consistent with our previous studies [20,49], the most dilated uterine lumen was seen in hCG-treated rats compared to the other three groups, and multiple cystic glands filled with large amounts of secretory fluid were found in hCG + insulin-treated rats (Fig. 5A). General histological evaluation of the uterine sections stained with H&E showed that the luminal epithelial cells remained cuboidal with similar thickness in saline-treated and insulin-treated rats, but increased luminal epithelial cell height and the appearance of vacuoles and the formation of multiple cell layers were observed in hCG + insulin-treated and hCG-treated rats (Fig. 5A). In line with previous results [62–64], immunochemical analysis revealed that the luminal and glandular epithelial cells exhibited greater GR immunoreactivity in the cytoplasm compared to the nucleus, which was in contrast to the predominantly nuclear GR expression in stromal cells in control rats (Fig. 5B). In addition, GR immunoreactivity was also observed in the myometrium and blood vessels (Fig. 5B). Quantitative data from Western blot analysis indicated that the expression of GRα and GRβ together with total GR was significantly decreased in hCG + insulin-treated rats compared to controls; however, no significant difference in GRα, GRβ, or total GR expression was found between saline-treated and hCG-treated rats or between saline-treated and insulin-treated rats (Fig. 5C). Similar to the ovary (Fig. 1D), the expression of *Fkbp51* mRNA was increased in the rat uterus compared to control rats regardless of whether the rat was treated with hCG, insulin, or a combination of the two (Fig. 5D). Unlike the ovary (Fig. 1D), however, the expression of *Fkbp52* mRNA was

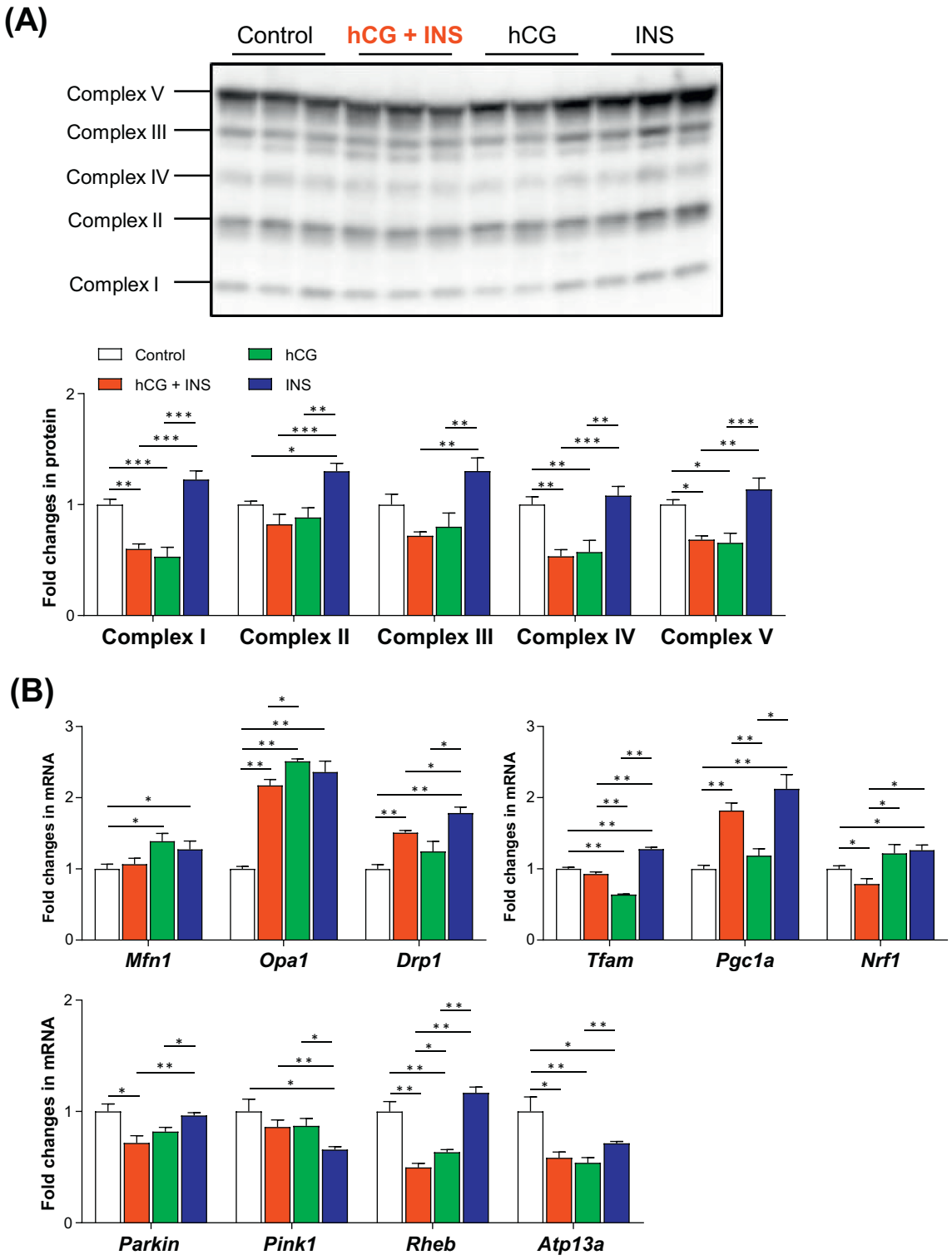

Fig. 2. Alteration of ovarian mitochondrial OXPHOS protein expression and key mitochondrial-related gene expression in rats treated chronically with hCG and/or insulin. (A) Regulation of OXPHOS protein expression in the ovary. Protein levels were analyzed by Western blotting (n = 9/group). (B) Regulation of genes that are related to mitochondrial fusion and fission, transcriptional activation, and mitophagy in the ovary. mRNA levels were determined by qRT-PCR (n = 6/group). In all plots, data are presented as means ± SEM. *p < 0.05, **p < 0.01, ***p < 0.001.

significantly higher in hCG-treated and insulin-treated rats compared to control rats (Fig. 5D). Furthermore, quantitative data from qRT-PCR indicated that the *Hsd11b1* mRNA level was increased in rats treated with hCG and/or insulin compared to controls, and a decreased *Hsd11b2* mRNA level was only seen in hCG-treated rats compared to control rats (Fig. 5E).

To investigate whether mitochondrial function and homeostasis were altered in the uterus or the ovary in response to hCG and insulin treatment, the expression of five respiratory protein complexes and a set of genes (*Mfn1*, *Opa1*, *Drp1*, *Tfam*, *Pgc1a*, *Nrf1*, *Parkin*, *Pink1*, *Rheb*, and *Atp13a*) was determined by Western blotting and qRT-PCR. As shown in Fig. 6A, while the expression of OXPHOS Complex I was

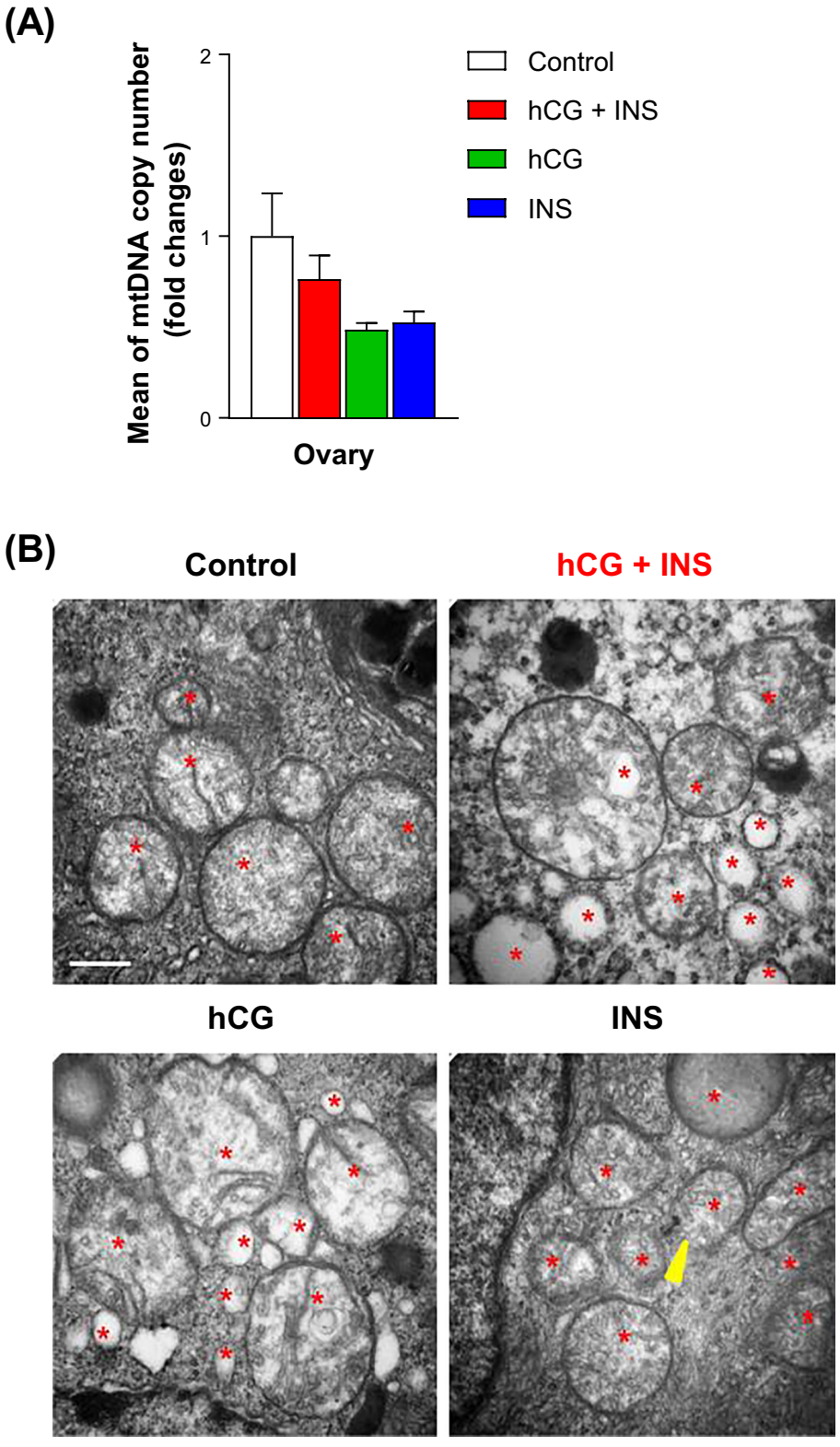

Fig. 3. Exposure of hCG or insulin alone or in combination alters ovarian mtDNA copy number and mitochondrial ultrastructure in rats. Ovarian mtDNA copy number from rats treated with saline, hCG + INS, hCG, or INS is shown (A, n = 6/group). Data are presented as means ± SEM. Electron micrographs show that mitochondria were found surrounding the nucleus in ovarian granulosa cells (B). Stars indicate the mitochondria, and arrowhead indicates the mitochondrial membrane rupture. Images are representative of two tissue replicates. Scale bars (500 nm) are indicated in the photomicrographs. INS, insulin.

decreased in hCG + insulin-treated and hCG-treated rats, Complexes III, IV, and V were only decreased in hCG + insulin-treated rats compared to controls rats. There were no significant changes in the five respiratory protein complexes between insulin-treated and control rats.

The levels of *Mfn1*, *Opa1*, *Drp1*, *Tfam*, *Pgc1a*, *Nrf1*, *Parkin*, and *Rheb* mRNAs, but not *Pink1* and *Atp13a* mRNAs, were increased in hCG + insulin-treated rats compared to controls rats (Fig. 6B). All measured gene levels were increased to some extent in hCG-treated and

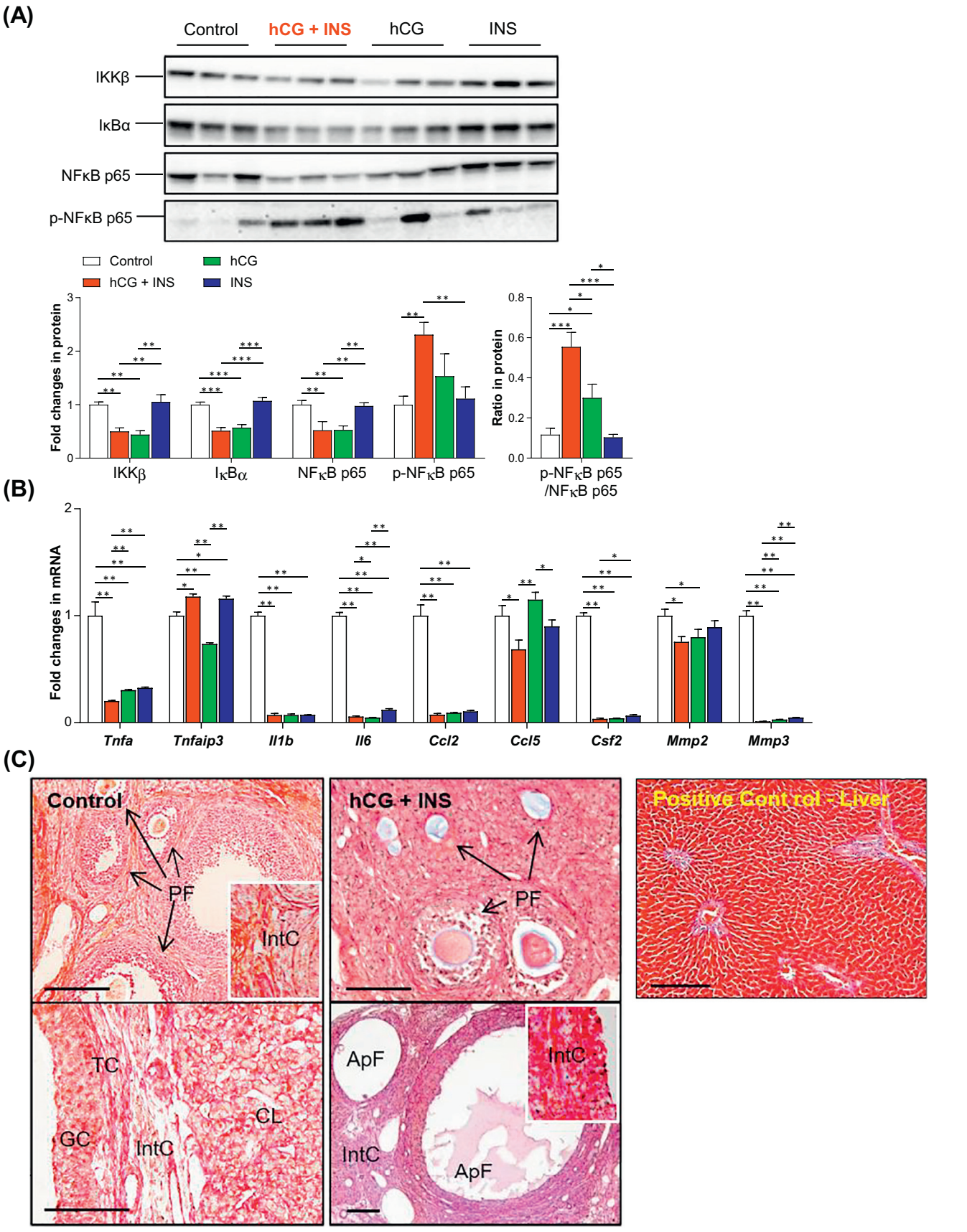

(caption on next page)

Fig. 4. Impaired ovarian NF-κB signaling mediates inflammation and collagen production in rats treated chronically with hCG and/or insulin. (A) Regulation of NF-κB signaling-related protein expression in the ovary. Protein levels were analyzed by Western blotting (n = 9/group). (B) Regulation of inflammatory gene expression in the ovary. mRNA levels were determined by qRT-PCR (n = 6/group). In all plots, data are presented as means ± SEM. *$p < 0.05$, **$p < 0.01$, ***$p < 0.001$. (C) Collagen production in the ovary. Representative images of Masson's trichrome staining in ovaries collected from rats treated with hCG and insulin. Aniline blue indicates collagen staining. PF, primary follicle; ApF, apoptotic follicle; CL, corpus luteum; GC, granulosa cells; TC, theca cells; IntC, interstitial cells. Scale bars (100 μm) are indicated in the photomicrographs.

insulin-treated rats compared to controls, indicating a similar gene expression pattern for hCG and insulin treatment (Fig. 6B). We further examined the ultrastructure of uterine epithelial cells by TEM to gain a better understanding of the effects of hCG and/or insulin on the uterus. As shown in Fig. 7, although no significant difference was seen in uterine mtDNA copy number between treatment and control rats (Fig. 7A), the mitochondria exhibited disrupted tubular cristae, blebbing, and decreased electron density in hCG + insulin-treated and hCG-treated rats (Fig. 7B).

Similar to the ovary (Fig. 4A), decreased IKKβ, IκBα, and total NFκB (p65) protein expression and increased p-NFκB (p65) protein expression and increased ratio of p-NFκB (p65) to total NFκB (p65) protein levels were observed in hCG + insulin-treated rats (Fig. 8A). In addition, we observed that while there was no change in any measured protein expression between insulin-treated rats and controls, total NFκB (p65) protein expression was decreased in hCG-treated rats compared to control rats (Fig. 8A). At the same time, increased *Tnfa*, *Tnfaip3*, *Ccl2*, *Ccl5*, and *Mmp3* mRNA expression and decreased *Il1b*, *Il6*, and *Mmp2* mRNA expression was observed in hCG + insulin-treated rats (Fig. 8B). Furthermore, while a similar regulatory pattern of *Tnfaip3*, *Il1b*, *Il6*, and *Ccl5* mRNA expression was seen in hCG-treated and insulin-treated rats, the expression of *Tnfa*, *Ccl2*, *Csf2*, *Mmp2*, and *Mmp3* mRNA was either increased or unchanged in hCG-treated rats compared to control rats (Fig. 8B). Lastly, Masson's trichrome staining showed that the deposition of uterine collagen was significantly increased in hCG + insulin-treated and insulin-treated rats compared to control rats, whereas uterine collagen deposition was significantly decreased in hCG-treated rats compared to control rats (Fig. 8C).

4. Discussion

Suppression of GR signaling in association with disturbed mitochondrial function and inflammation in the ovary and uterus caused by hyperandrogenism and insulin resistance has never to our knowledge been investigated *in vivo*. Consistent with previous studies [20,22,46,48,49], we found that concomitant treatment with hCG and insulin mimicking the main pathologies of PCOS causes pronounced morphological and cellular alterations in the ovary and uterus such as the formation of ovarian cystic follicles and multiple cystic glands filled with large amounts of secretory fluid as well as increased luminal epithelial cell layers. In addition to morphological analyses, we report the following main findings. (1) Compared to controls, rats treated with hCG and insulin exhibited decreased protein expression of the two GR isoforms and increased *Fkbp51* mRNA expression in both the ovary and the uterus. (2) Co-treatment with hCG and insulin resulted in an opposite regulatory pattern of *Hsd11b1* of *Hsd11b2* mRNAs in the two tissues, which is likely due to different effects of hCG and insulin. (3) Decreased expression of the respiratory protein complexes paralleled the increased expression of key genes responsible for mitochondrial fusion, fission, and biogenesis in both tissues. (4) Although there was no difference of mtDNA copy number between control and treatment groups, TEM revealed abnormal mitochondrial morphology in ovarian granulosa cells and uterine epithelial cells treated with hCG alone or in combination with insulin. (5) Increased expression of NFκB signaling proteins and *Tnfaip3*, as well as decreased expression of *Il1b*, *Il6*, and *Mmp2* mRNAs, was similar in the PCOS-like ovary and uterus, while the opposite regulation of *Tnfa*, *Ccl2*, *Ccl5*, and *Mmp3* mRNA expression was observed in the two tissues under the same conditions. (6) The increase in collagen deposition was similar in the two tissues under conditions of hyperandrogenism and insulin resistance.

In this study, we observed similar regulatory patterns of GR protein isoform expression in both the ovary and uterus after stimulation with hCG and insulin. While elevated E3 ubiquitin ligases, the key components of the ubiquitin-proteasome system that stabilizes multiple proteins, are critical for the development of insulin resistance [65], Lim and colleagues have reported that increased AR ubiquitination – which results in inhibition of AR transcriptional activity and decreases its stability – is involved in the follicular growth arrest seen in the 5α-dihydrotestosterone-induced PCOS-like rat ovary [66]. In addition, alterations in protein ubiquitination have also been reported to have negative effects on GR expression and activity *in vivo* [67], and uterine GR knockout studies have shown that GR positively regulates embryo implantation and decidualization [14]. We therefore speculate that down-regulation of GR protein levels is due to increased GR ubiquitination under conditions of hyperandrogenism and insulin resistance and that this results in negative consequences such as increased NFκB-regulated inflammation in the ovary and uterus. Because deciphering the molecular mechanisms of hyperandrogenism and insulin resistance *in vivo* is essential to understanding the possible etiologies and therapeutic approaches for PCOS, further investigations are needed to better understand how GR signaling directly contributes to the development of ovarian and uterine dysfunction in PCOS patients.

This study further demonstrates the association between two *Hsd11b* mRNAs and hyperandrogenism and insulin resistance in the rat ovary and uterus. We showed that concomitant treatment with hCG and insulin decreased *Hsd11b1* mRNA expression and increased *Hsd11b2* mRNA expression in the ovary. In stark contrast to the ovary, the same treatment increased *Hsd11b1* mRNA expression but did not change *Hsd11b2* mRNA expression in the uterus. Given the opposing roles of *Hsd11b1* and *Hsd11b2* in the regulation of local active cortisol (corticosterone in rodents) concentrations [34], it is tempting to speculate from these observations that, in contrast to the uterus, the activation of 11-dehydrocorticosterone to corticosterone is decreased in the ovary under conditions of hyperandrogenism and insulin resistance. However, this outcome is quite different to what is seen in the human data. In hyperandrogenic PCOS patients, elevated *Hsd11b1* mRNA levels in granulosa cells are closely linked to ovarian insulin resistance, whereas lower *Hsd11b2* mRNA and protein levels contribute to endometrial insulin resistance [23,24]. Despite the presence of similar, different, or even opposite regulation and localization of the two 11βHSD isoforms in the ovarian and endometrial cells [10,11,34], evidence for their physiological roles in the ovary and uterus is lacking. Additionally, there are differences in the regulation of ovarian hormone receptors such as AR between PCOS patients and PCOS-like animal models [68]. Although abnormal cortisol metabolism has been shown in some PCOS patients [29,30], GR can be activated by estrogens in addition to glucocorticoids in the uterus [11]. However, because our findings are from observing only a single time point, the possibility that aberrant regulation of the two *Hsd11b* isoform mRNAs depends on local endocrine environments in the ovary and uterus during the progression of hyperandrogenism and insulin resistance remains entirely speculative.

Mitochondria are essential not only for generation of ATP by aerobic respiration, but also for steroidogenesis through mitochondrial cholesterol transport and metabolism [69]. Although the precise mechanism underlying mitochondria-regulated ovarian and uterine cell function is uncertain, it is becoming increasingly evident that impaired

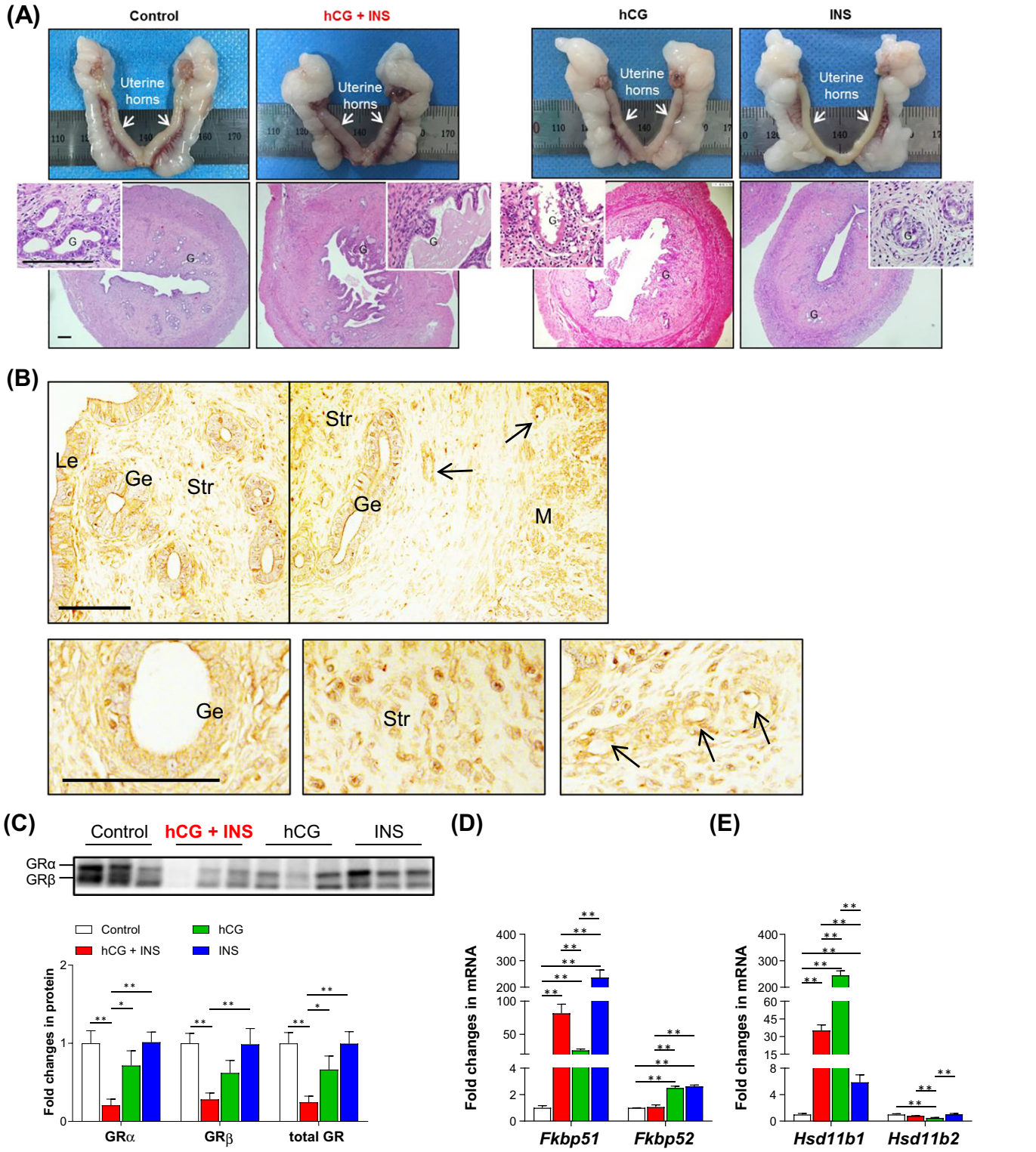

Fig. 5. Uterine defects and impaired GR, *Fkbp5*, and *Hsd11b* expression in rats treated chronically with hCG and/or insulin. (A) Representative photographs of uteri and images of H&E staining in the uterus. Scale bars (200 μm) are indicated in the photomicrographs. (B) Representative photomicrographs of immunohistochemical staining for uterine GR in control rats. Arrows indicate the uterine blood vessels. Le, luminal epithelial cells; G, glands; Ge, glandular epithelial cells; Str, stromal cells; M, myometrium. Scale bars (100 μm) are indicated in the photomicrographs. (C) Regulation of GR protein expression in the uterus. Protein levels were analyzed by Western blotting (n = 8 or 9/group). (D and E) Regulation of *Fkbp5* and *Hsd11b* gene expression in the uterus. mRNA levels were determined by qRT-PCR (n = 8/group). In all plots, data are presented as means ± SEM. *$p < 0.05$, **$p < 0.01$.

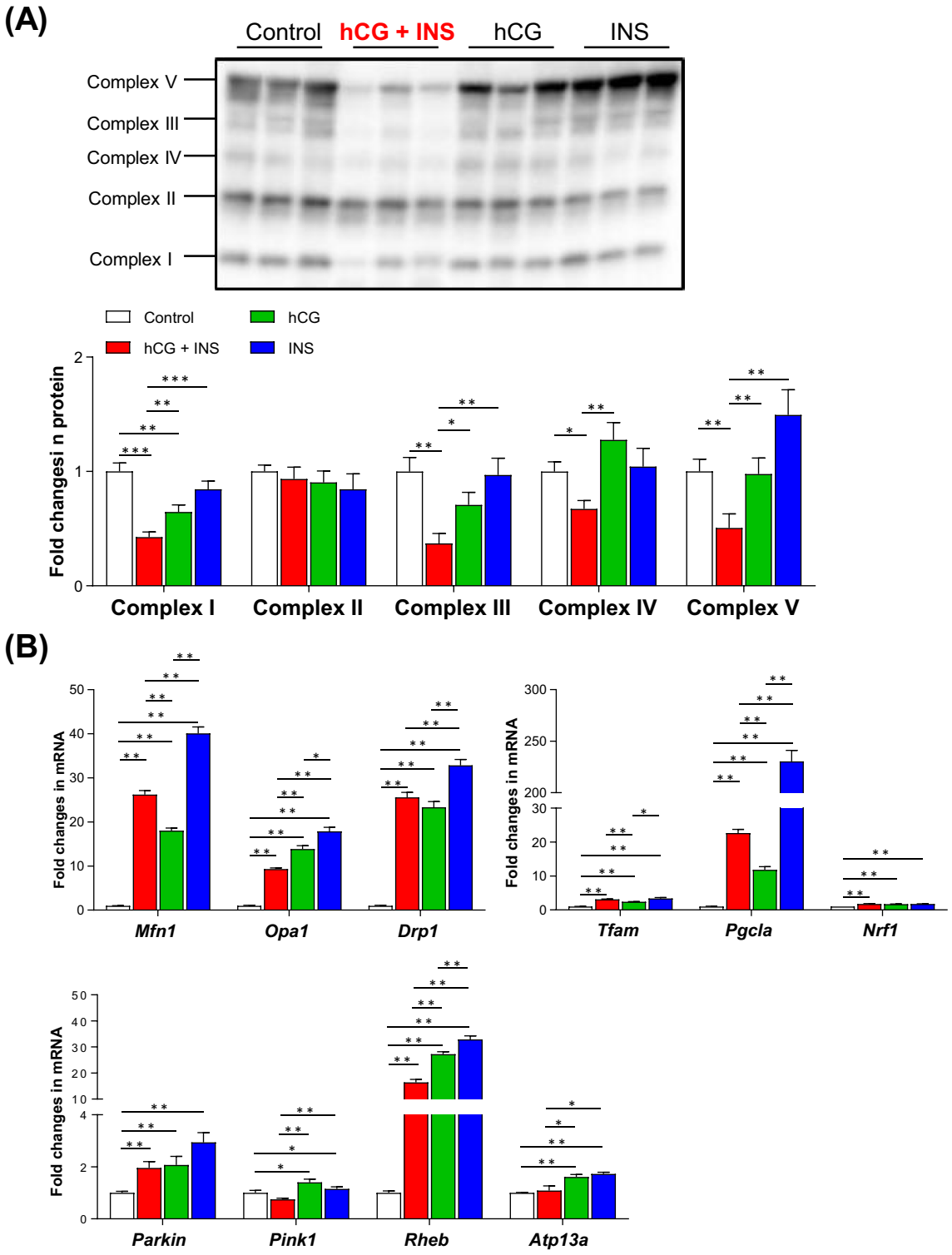

Fig. 6. Alteration of uterine mitochondrial OXPHOS protein expression and key mitochondrial-related gene expression in rats treated chronically with hCG and/or insulin. (A) Regulation of OXPHOS protein expression in the uterus. Protein levels were analyzed by Western blotting (n = 8 or 9/group). (B) Regulation of genes that are related to mitochondrial fusion and fission, transcriptional activation, and mitophagy in the uterus. mRNA levels were determined by qRT-PCR (n = 8/group). In all plots, data are presented as means ± SEM. *p < 0.05, **p < 0.01, ***p < 0.001.

mitochondrial function is seen in PCOS patients and PCOS-like animals [26,39–45]. We found that rats co-treated with hCG and insulin had reduced levels of OXPHOS-related proteins (NADH dehydrogenase, cytochrome *c* oxidase, and ATP synthase) in the ovary and uterus. This observation indicates that the mitochondrial respiratory capacity was affected by hyperandrogenism and insulin resistance, thus suggesting that these conditions cause the mitochondria-mediated metabolic defects seen in the two tissues. Unexpectedly, in parallel to the GR down-regulation, the same animals exhibited increased expression of genes involved in mitochondrial fusion (*Opa1*), fission (*Drp1*), and biogenesis (*Pgc1a*) in both tissues. In addition, we also showed that expression of the mitophagic genes *Parkin* and *Rheb* was decreased in the ovary,

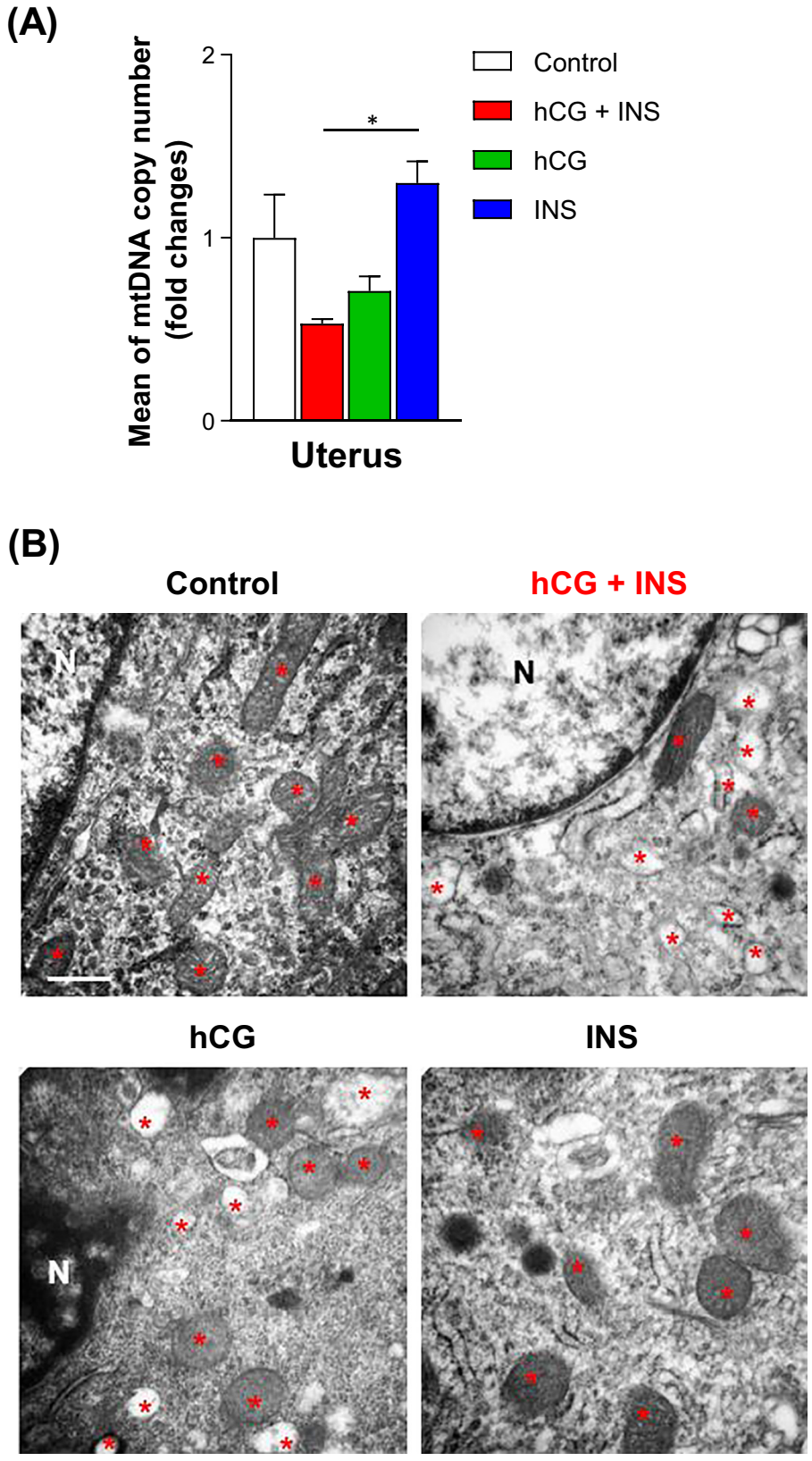

Fig. 7. Exposure of hCG or insulin alone or in combination alters uterine mtDNA copy number and mitochondrial ultrastructure in rats. Uterine mtDNA copy number from rats treated with saline, hCG + INS, hCG, or INS is shown (A, n = 6/group). Data are presented as means ± SEM. *$p < 0.05$. Electron micrographs show that mitochondria were found surrounding the nucleus in uterine epithelial cells (B). The stars indicate the mitochondria. Images are representative of two tissue replicates. Scale bars (500 nm) are indicated in the photomicrographs. INS, insulin; N, nucleus.

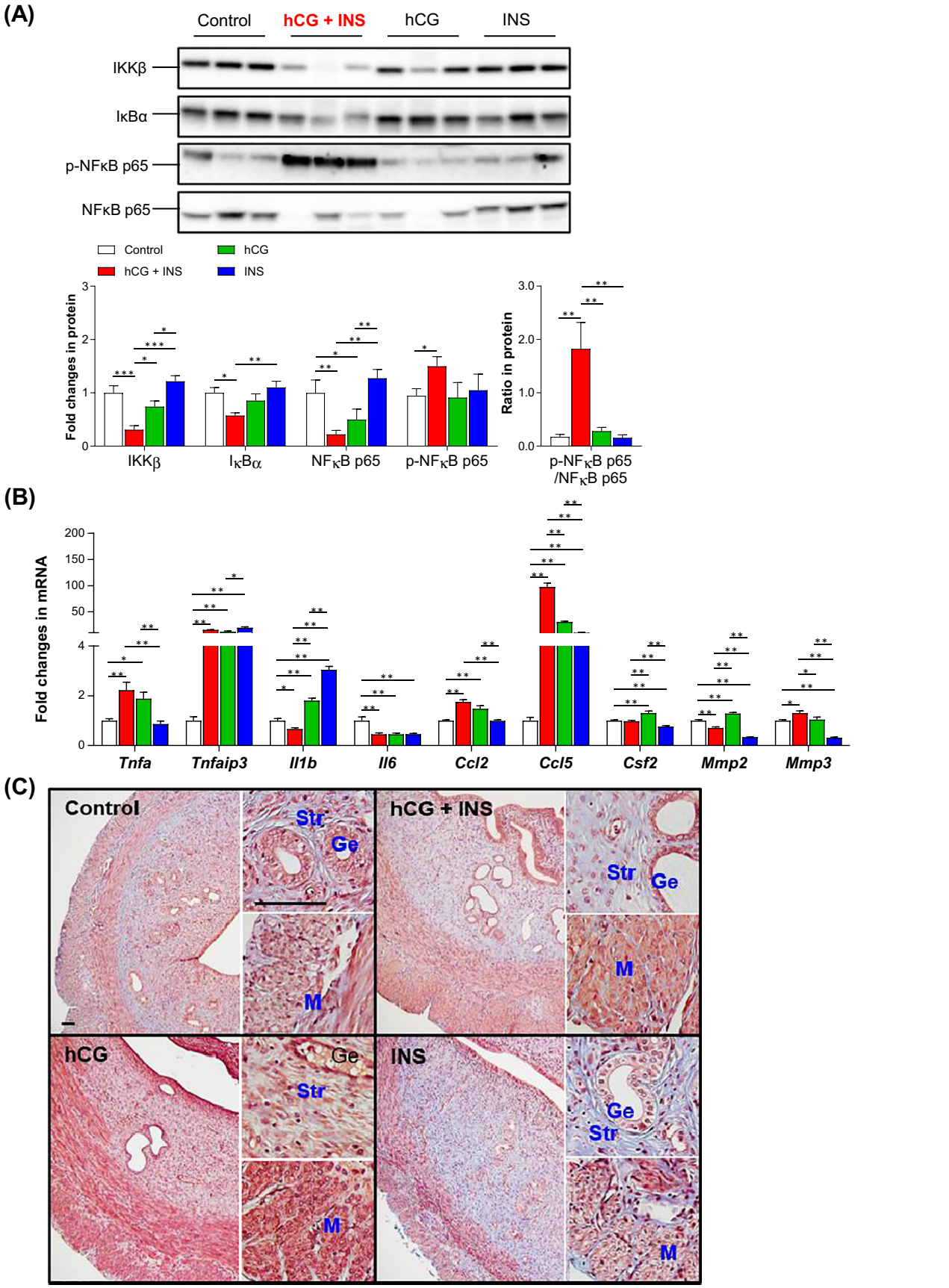

(caption on next page)

Fig. 8. Impaired uterine NF-κB signaling mediates inflammation and collagen production in rats treated chronically with hCG and/or insulin. (A) Regulation of NF-κB signaling-related protein expression in the uterus. Protein levels were analyzed by Western blotting (n = 8 or 9/group). (B) Regulation of inflammation-related gene expression in the uterus. mRNA levels were determined by qRT-PCR (n = 8/group). In all plots, data are presented as means ± SEM. *p < 0.05, **p < 0.01, ***p < 0.001. (C) Collagen production in the uterus. Representative images of Masson's trichrome staining in ovaries collected from rats treated with hCG and insulin. Aniline blue indicates collagen staining. Ge, glandular epithelial cells; Str, stromal cells; M, myometrium. Scale bars (100 μm) are indicated in the photomicrographs.

whereas the same gene expression was increased in the uterus. Healthy mitochondrial function is dependent on the fusion-fission cycle, while damaged and unwanted mitochondria are removed by mitophagy [58]. Based on qRT-PCR and Western blot analyses using the ovarian and uterine homogenates, we cannot rule out the possibility that different mechanisms are responsible for RNA turnover and translational control of protein turnover and abundance in the ovary and uterus in response to the hormonal milieu [20,40]. However, it is worth noting that the decrease in mitochondrial respiratory capacity might stimulate the mitochondrial fusion-fission cycle and biogenesis through a complementary or adaptive effect during the progression of hyperandrogenism and insulin resistance.

Although GR acts as both an enhancer and inhibitor for controlling a large number of transcriptional pathways, diverse mechanistic models have been proposed for the specific effects of GR repression on NFκB activity *in vitro* [56,59]. We highlight how the conditions of hyperandrogenism and insulin resistance suppressed GR protein expression and activated NFκB signaling in the ovary and uterus. Numerous clinical studies have reported that androgen excess, hyperinsulinemia, and systemic inflammation often co-exist in PCOS patients [72]. Notably, PCOS patients display significant activation of NFκB signaling in association with elevated inflammation in ovarian granulosa cells and endometrial cells [70–72]. Despite the overlapping and distinct cytokine and chemokine gene expression between the ovary and uterus, PCOS-like rats showed aberrant regulation of *Mmp2* and *Mmp3* mRNAs leading to increased collagen deposition in both tissues. In line with our findings, Henmi and colleagues have reported that elevated ovarian Mmp2 protein expression modulates collagen synthesis in dehydroepiandrosterone-induced PCOS-like rats [73]. Taken together, the present study suggests that the GR–NFκB signaling axis probably plays a contributing role in triggering chronic inflammation ultimately resulting in ovarian and uterine dysfunction under the conditions of hyperandrogenism and insulin resistance. Our understanding of the molecular mechanism and biological function of GR has increased. However, how and when the suppression of GR signaling induces ovarian and uterine dysfunctions in PCOS patients warrants further investigation.

Our results also demonstrated that rats treated with hCG alone or insulin alone exhibited a distinct regulatory pattern of several genes in the ovary and uterus. Moreover, even stronger effects were seen for hCG- and insulin-targeted gene/protein expression than in hCG + insulin-treated rats. These findings suggest that the regulation of ovarian and uterine gene/protein expression responses to hCG and insulin stimulation is complex. At the cellular level, it is generally accepted that the diverse effects of hCG, an analog of luteinizing hormone (LH), and insulin are mainly mediated by interactions with LH receptor (LHR) and insulin receptor (IR), respectively [74,75]. We recognize that both LHR and IR are expressed in rat ovarian and uterine cells [49,76–79], and it is likely that the regulation of ovarian and uterine gene/protein expression is both direct and hormone-specific. However, it has been proposed that at the systemic level, interactions between the LH/LHR and insulin/IR signaling pathways contribute to the disrupted ovarian function under PCOS conditions [80]. Further research is required to determine whether the two hormones share similar regulatory mechanisms in the ovary and uterus and if there is causal relationship between disruptions in their activity and the pathogenesis of PCOS. The present study only profiled hCG- and insulin-regulated genes and proteins at a single point in time in rats mimicking a PCOS-like state, and it is possible that either or both hormones might regulate the spatial and temporal expression of genes/proteins in the ovary and uterus. Thus longitudinal studies of hormone regulation would be of great interest.

5. Conclusion

Collectively, for the first time our data reinforce the importance of PCOS-related hyperandrogenism and insulin resistance for aberrant GR signaling in association with changes in mitochondrial function and homeostasis as well as NFκB-regulated inflammation in the rat ovary and uterus. Of note, the opposite regulation between OXPHOS proteins and genes that act as the key regulators for mitochondrial fusion, fission, and biogenesis in PCOS-like rats suggests that such compensatory or adaptive mechanisms probably help protect ovarian and uterine cells against hyperandrogenism and insulin resistance-induced damage. Although several PCOS-like rat models have been developed [81], no perfect animal model exists that can account for all aspects of human PCOS. We and others have used chronic treatment with hCG and insulin to create an *in vivo* rodent model for the onset and development of PCOS-like phenotypes, but further studies using various PCOS-like animal models are needed to confirm our current initial observations. Given the fact that no means exist to predict or prevent the onset and lifelong consequences of PCOS in humans [68], the identification of the relationships between different molecular mechanisms and PCOS phenotypes, including elucidation of the regulation of GR signaling under conditions of hyperandrogenism and insulin resistance, will provide insights into how ovarian and uterine cells respond and adapt to the pathological conditions of PCOS.

Abbreviations

Fkbp51	FK506 binding protein 5
GR	glucocorticoid receptor
Hsd11b	11β-hydroxysteroid dehydrogenase
IκBα	nuclear factor of kappa light polypeptide gene enhancer in B-cells inhibitor alpha
IKKβ	inhibitor of NFkB kinase complex β
Mmp2	matrix metallopeptidase 2
NF-κB	nuclear factor kappa-light-chain-enhancer of activated B cells
Nrf1	nuclear respiratory factor 1
OXPHOS	oxidative phosphorylation
PCOS	polycystic ovary syndrome
Pgc1a	peroxisome proliferator-activated receptor gamma coactivator 1 alpha
Tfam	mitochondrial transcription factor A
Tnfa	tumor necrosis factor alpha

Authors' contributions

LRS contributed to study conceptualization, supervision, and original draft; MH, YZ, XG, WJ, GL, JZ, PC, JL, WL, and LRS contributed to the development of methodology, acquisition of data, and conducting the experiments; MH, YZ, and LRS contributed to the analysis and interpretation of the data; MH, MB, LRS, and HB contributed to the review and editing of the manuscript; XW, HM, MB, LRS, and HB, contributed to the scientific oversight and guidance; and YZ, LRS, and HB provided administrative, technical, and material support. All authors have read and approved the final version of the manuscript.

Funding

This study was financed by grants from the Swedish Medical Research Council (grant number 10380), the Swedish state under the agreement between the Swedish government and the county councils-the ALF-agreement (grant number ALFGBG-147791), Jane and Dan Olssons Foundation, the Knut and Alice Wallenberg Foundation, and the Adlerbert Research Foundation to HB and LRS as well as by grants from the National Natural Science Foundation of China (grant number 81774136), the Project of Science Foundation by Heilongjiang University of Chinese Medicine, the Project of Excellent Innovation Talents by Heilongjiang University of Chinese Medicine, and the Science Initiation Foundation for Post-doctoral Researchers Settled in Heilongjiang Province to YZ. The Guangzhou Medical University High-level University Construction Talents Fund (grant number B185006010046) supported MH.

Declaration of Competing Interest

The authors indicate no potential conflicts of interest.

References

[1] D. Lizneva, L. Suturina, W. Walker, S. Brakta, L. Gavrilova-Jordan, R. Azziz, Criteria, prevalence, and phenotypes of polycystic ovary syndrome, Fertil. Steril. 106 (2016) 6–15.
[2] X. Li, Y. Feng, J.F. Lin, H. Billig, R. Shao, Endometrial progesterone resistance and PCOS, J. Biomed. Sci. 21 (2014) 2.
[3] L.G. Cooney, A. Dokras, Beyond fertility: polycystic ovary syndrome and long-term health, Fertil. Steril. 110 (2018) 794–809.
[4] R. Shao, X. Li, Y. Feng, J.F. Lin, H. Billig, Direct effects of metformin in the endometrium: a hypothetical mechanism for the treatment of women with PCOS and endometrial carcinoma, J. Exp. Clin. Cancer Res. 33 (2014) 41.
[5] R. Homburg, Management of infertility and prevention of ovarian hyperstimulation in women with polycystic ovary syndrome, Best Pract. Res. Clin. Obstet. Gynaecol. 18 (2004) 773–788.
[6] P. Chakraborty, S.K. Goswami, S. Rajani, S. Sharma, S.N. Kabir, B. Chakravarty, K. Jana, Recurrent pregnancy loss in polycystic ovary syndrome: role of hyperhomocysteinemia and insulin resistance, PLoS One 8 (2013) e64446.
[7] R.L. Rosenfield, D.A. Ehrmann, The pathogenesis of polycystic ovary syndrome (PCOS): the hypothesis of PCOS as functional ovarian hyperandrogenism revisited, Endocr. Rev. 37 (2016) 467–520.
[8] R. Azziz, E. Carmina, Z. Chen, A. Dunaif, J.S. Laven, R.S. Legro, D. Lizneva, B. Natterson-Horowtiz, H.J. Teede, B.O. Yildiz, Polycystic ovary syndrome, Nat. Rev. Dis. Primer 2 (2016) 16057.
[9] H.F. Escobar-Morreale, Polycystic ovary syndrome: definition, aetiology, diagnosis and treatment, Nat. Rev. Endocrinol. 14 (2018) 270–284.
[10] S. Whirledge, D.B. DeFranco, Glucocorticoid signaling in health and disease: insights from tissue-specific GR knockout mice, Endocrinology 159 (2018) 46–64.
[11] S. Whirledge, J.A. Cidlowski, A role for glucocorticoids in stress-impaired reproduction: beyond the hypothalamus and pituitary, Endocrinology 154 (2013) 4450–4468.
[12] M. Tetsuka, Actions of glucocorticoid and their regulatory mechanisms in the ovary, Anim. Sci. J. 78 (2007) 112–120.
[13] H.O. Critchley, P.T. Saunders, Hormone receptor dynamics in a receptive human endometrium, Reprod. Sci. 16 (2009) 191–199.
[14] S.D. Whirledge, R.H. Oakley, P.H. Myers, J.P. Lydon, F. DeMayo, J.A. Cidlowski, Uterine glucocorticoid receptors are critical for fertility in mice through control of embryo implantation and decidualization, Proc. Natl. Acad. Sci. U. S. A. 112 (2015) 15166–15171.
[15] P.Z. Zhou, Y.M. Zhu, G.H. Zou, Y.X. Sun, X.L. Xiu, X. Huang, Q.H. Zhang, Relationship between glucocorticoids and insulin resistance in healthy individuals, Med. Sci. Monit. 22 (2016) 1887–1894.
[16] T. Kuo, A. McQueen, T.C. Chen, J.C. Wang, Regulation of glucose homeostasis by glucocorticoids, Adv. Exp. Med. Biol. 872 (2015) 99–126.
[17] M. Belani, N. Purohit, P. Pillai, S. Gupta, S. Gupta, Modulation of steroidogenic pathway in rat granulosa cells with subclinical Cd exposure and insulin resistance: an impact on female fertility, Biomed. Res. Int. 2014 (2014) 460251.
[18] K.S. Hackbart, P.M. Cunha, R.K. Meyer, M.C. Wiltbank, Effect of glucocorticoid-induced insulin resistance on follicle development and ovulation, Biol. Reprod. 88 (2013) 153.
[19] L. Kong, Q. Wang, J. Jin, Z. Xiang, T. Chen, S. Shen, H. Wang, Q. Gao, Y. Wang, Insulin resistance enhances the mitogen-activated protein kinase signaling pathway in ovarian granulosa cells, PLoS One 12 (2017) e0188029.
[20] Y. Zhang, X. Sun, X. Sun, F. Meng, M. Hu, X. Li, W. Li, X.K. Wu, M. Brännström, R. Shao, H. Billig, Molecular characterization of insulin resistance and glycolytic metabolism in the rat uterus, Sci. Rep. 6 (2016) 30679.
[21] S. Andrisse, K. Billings, P. Xue, S. Wu, Insulin signaling displayed a differential tissue-specific response to low-dose dihydrotestosterone in female mice, Am. J. Physiol. Endocrinol. Metab. 314 (2018) E353–E365.
[22] D.F. Restuccia, D. Hynx, B.A. Hemmings, Loss of PKBbeta/Akt2 predisposes mice to ovarian cyst formation and increases the severity of polycystic ovary formation in vivo, Dis. Model. Mech. 5 (2012) 403–411.
[23] J. Qi, W. Wang, Q. Zhu, Y. He, Y. Lu, Y. Wang, X. Li, Z.J. Chen, Y. Sun, Local cortisol elevation contributes to endometrial insulin resistance in polycystic ovary syndrome, J. Clin. Endocrinol. Metab. 103 (2018) 2457–2467.
[24] Q. Zhu, R. Zuo, Y. He, Y. Wang, Z.J. Chen, Y. Sun, K. Sun, Local regeneration of cortisol by 11beta-HSD1 contributes to insulin resistance of the granulosa cells in PCOS, J. Clin. Endocrinol. Metab. 101 (2016) 2168–2177.
[25] X. Li, B. Pishdari, P. Cui, M. Hu, H.P. Yang, Y.R. Guo, H.Y. Jiang, Y. Feng, H. Billig, R. Shao, Regulation of androgen receptor expression alters AMPK phosphorylation in the endometrium: in vivo and in vitro studies in women with polycystic ovary syndrome, Int. J. Biol. Sci. 11 (2015) 1376–1389.
[26] T. Wang, J. Zhang, M. Hu, Y. Zhang, P. Cui, X. Li, J. Li, E. Vestin, M. Brannstrom, L.R. Shao, H. Billig, Differential expression patterns of glycolytic enzymes and mitochondria-dependent apoptosis in PCOS patients with endometrial hyperplasia, an early hallmark of endometrial cancer, in vivo and the impact of metformin in vitro, Int. J. Biol. Sci. 15 (2019) 714–725.
[27] D. Dewailly, G. Robin, M. Peigne, C. Decanter, P. Pigny, S. Catteau-Jonard, Interactions between androgens, FSH, anti-Mullerian hormone and estradiol during folliculogenesis in the human normal and polycystic ovary, Hum. Reprod. Update 22 (2016) 709–724.
[28] F. Claessens, S. Joniau, C. Helsen, Comparing the rules of engagement of androgen and glucocorticoid receptors, Cell. Mol. Life Sci. 74 (2017) 2217–2228.
[29] T. Tsilchorozidou, J.W. Honour, G.S. Conway, Altered cortisol metabolism in polycystic ovary syndrome: insulin enhances 5alpha-reduction but not the elevated adrenal steroid production rates, J. Clin. Endocrinol. Metab. 88 (2003) 5907–5913.
[30] D.A. Vassiliadi, T.M. Barber, B.A. Hughes, M.I. McCarthy, J.A. Wass, S. Franks, P. Nightingale, J.W. Tomlinson, W. Arlt, P.M. Stewart, Increased 5 alpha-reductase activity and adrenocortical drive in women with polycystic ovary syndrome, J. Clin. Endocrinol. Metab. 94 (2009) 3558–3566.
[31] A. Gambineri, F. Fanelli, F. Tomassoni, A. Munarini, U. Pagotto, R. Andrew, B.R. Walker, R. Pasquali, Tissue-specific dysregulation of 11beta-hydroxysteroid dehydrogenase type 1 in overweight/obese women with polycystic ovary syndrome compared with weight-matched controls, Eur. J. Endocrinol. 171 (2014) 47–57.
[32] L.L. Gathercole, G.G. Lavery, S.A. Morgan, M.S. Cooper, A.J. Sinclair, J.W. Tomlinson, P.M. Stewart, 11beta-Hydroxysteroid dehydrogenase 1: translational and therapeutic aspects, Endocr. Rev. 34 (2013) 525–555.
[33] P.F. Svendsen, S. Madsbad, L. Nilas, S.K. Paulsen, S.B. Pedersen, Expression of 11beta-hydroxysteroid dehydrogenase 1 and 2 in subcutaneous adipose tissue of lean and obese women with and without polycystic ovary syndrome, Int. J. Obes. 33 (2009) 1249–1256.
[34] K. Chapman, M. Holmes, J. Seckl, 11beta-hydroxysteroid dehydrogenases: intracellular gate-keepers of tissue glucocorticoid action, Physiol. Rev. 93 (2013) 1139–1206.
[35] H.E. Lapp, A.A. Bartlett, R.G. Hunter, Stress and glucocorticoid receptor regulation of mitochondrial gene expression, J. Mol. Endocrinol. 62 (2019) R121–R128.
[36] M. Benkhalifa, Y.J. Ferreira, H. Chahine, N. Louanjli, P. Miron, P. Merviel, H. Copin, Mitochondria: participation to infertility as source of energy and cause of senescence, Int. J. Biochem. Cell Biol. 55 (2014) 60–64.
[37] R.G. Hunter, M. Seligsohn, T.G. Rubin, B.B. Griffiths, Y. Ozdemir, D.W. Pfaff, N.A. Datson, B.S. McEwen, Stress and corticosteroids regulate rat hippocampal mitochondrial DNA gene expression via the glucocorticoid receptor, Proc. Natl. Acad. Sci. U. S. A. 113 (2016) 9099–9104.
[38] A.M. Psarra, C.E. Sekeris, Glucocorticoids induce mitochondrial gene transcription in HepG2 cells: role of the mitochondrial glucocorticoid receptor, Biochim. Biophys. Acta 1813 (2011) 1814–1821.
[39] Y. Ding, Z. Jiang, B. Xia, L. Zhang, C. Zhang, J. Leng, Mitochondria-targeted antioxidant therapy for an animal model of PCOS-IR, Int. J. Mol. Med. 43 (2019) 316–324.
[40] M. Hu, Y. Zhang, X. Guo, W. Jia, G. Liu, J. Zhang, J. Li, P. Cui, A.N. Sferruzzi-Perri, Y. Han, X. Wu, H. Ma, M. Brannstrom, L.R. Shao, H. Billig, Hyperandrogenism and insulin resistance induce gravid uterine defects in association with mitochondrial dysfunction and aberrant ROS production, Am. J. Physiol. Endocrinol. Metab. 316 (2019) E794–E809.
[41] Y. Zhang, F. Meng, X. Sun, X. Sun, M. Hu, P. Cui, E. Vestin, X. Li, W. Li, X.K. Wu, J.O. Jansson, L.R. Shao, H. Billig, Hyperandrogenism and insulin resistance contribute to hepatic steatosis and inflammation in female rat liver, Oncotarget 9 (2018) 18180–18197.
[42] M. Cree-Green, H. Rahat, B.R. Newcomer, B.C. Bergman, M.S. Brown, G.V. Coe, L. Newnes, Y. Garcia-Reyes, S. Bacon, J.E. Thurston, L. Pyle, A. Scherzinger, K.J. Nadeau, Insulin resistance, hyperinsulinemia, and mitochondria dysfunction in nonobese girls with polycystic ovarian syndrome, J. Endocr. Soc. 1 (2017) 931–944.
[43] H. Wang, X. Wang, Y. Zhu, F. Chen, Y. Sun, X. Han, Increased androgen levels in rats impair glucose-stimulated insulin secretion through disruption of pancreatic beta cell mitochondrial function, J. Steroid Biochem. Mol. Biol. 154 (2015) 254–266.
[44] H. Zhao, Y. Zhao, T. Li, M. Li, J. Li, R. Li, P. Liu, Y. Yu, J. Qiao, Metabolism alteration in follicular niche: the nexus among intermediary metabolism, mitochondrial function, and classic polycystic ovary syndrome, Free Radic. Biol. Med. 86 (2015) 295–307.
[45] E.S. Selen, Z. Bolandnazar, M. Tonelli, D.E. Butz, J.A. Haviland, W.P. Porter, F.M. Assadi-Porter, NMR metabolomics show evidence for mitochondrial oxidative stress in a mouse model of polycystic ovary syndrome, J. Proteome Res. 14 (2015) 3284–3291.

[46] M.H. Lima, L.C. Souza, L.C. Caperuto, E. Bevilacqua, A.L. Gasparetti, R. Zanuto, M.J. Saad, C.R. Carvalho, Up-regulation of the phosphatidylinositol 3-kinase/protein kinase B pathway in the ovary of rats by chronic treatment with hCG and insulin, J. Endocrinol. 190 (2006) 451–459.
[47] Y. Yang, H. Jiang, L. Xiao, X. Yang, MicroRNA-33b-5p is overexpressed and inhibits GLUT4 by targeting HMGA2 in polycystic ovarian syndrome: an in vivo and in vitro study, Oncol. Rep. 39 (2018) 3073–3085.
[48] M. Hu, Y. Zhang, J. Feng, X. Xu, J. Zhang, W. Zhao, X. Guo, J. Li, E. Vestin, P. Cui, X. Li, X.K. Wu, M. Brannstrom, L.R. Shao, H. Billig, Uterine progesterone signaling is a target for metformin therapy in PCOS-like rats, J. Endocrinol. 237 (2018) 123–137.
[49] Y. Zhang, M. Hu, F. Meng, X. Sun, H. Xu, J. Zhang, P. Cui, N. Morina, X. Li, W. Li, X.K. Wu, M. Brannstrom, R. Shao, H. Billig, Metformin ameliorates uterine defects in a rat model of polycystic ovary syndrome, EBioMedicine 18 (2017) 157–170.
[50] Y. Chen, J. Qiao, L.Y. Yan, S. Huang, P.L. Zhao, J. Yan, Selective impairment in glycogen synthase kinase-3 and mitogen-activated protein kinase phosphorylation: comparisons with the hyperandrogenic and the hyperinsulinemic rats, Fertil. Steril. 92 (2009) 1447–1455.
[51] H. Li, Y. Chen, L.Y. Yan, J. Qiao, Increased expression of P450scc and CYP17 in development of endogenous hyperandrogenism in a rat model of PCOS, Endocrine 43 (2013) 184–190.
[52] Y. Feng, B. Weijdegard, T. Wang, E. Egecioglu, J. Fernandez-Rodriguez, I. Huhtaniemi, E. Stener-Victorin, H. Billig, R. Shao, Spatiotemporal expression of androgen receptors in the female rat brain during the oestrous cycle and the impact of exogenous androgen administration: a comparison with gonadally intact males, Mol. Cell. Endocrinol. 321 (2010) 161–174.
[53] A. Razmara, S.P. Duckles, D.N. Krause, V. Procaccio, Estrogen suppresses brain mitochondrial oxidative stress in female and male rats, Brain Res. 1176 (2007) 71–81.
[54] Y. Zhang, W. Zhao, H. Xu, M. Hu, X. Guo, W. Jia, G. Liu, J. Li, P. Cui, S. Lager, A.N. Sferruzzi-Perri, W. Li, X.K. Wu, Y. Han, M. Brannstrom, L.R. Shao, H. Billig, Hyperandrogenism and insulin resistance-induced fetal loss: evidence for placental mitochondrial abnormalities and elevated ROS production in pregnant rats that mimic the clinical features of PCOS, J. Physiol. (2019) (In press).
[55] N.K. Kuscu, F. Koyuncu, K. Ozbilgin, S. Inan, I. Tuglu, O. Karaer, Insulin: does it induce follicular arrest in the rat ovary? Gynecol. Endocrinol. 16 (2002) 361–364.
[56] M. Bekhbat, S.A. Rowson, G.N. Neigh, Checks and balances: the glucocorticoid receptor and NFkB in good times and bad, Front. Neuroendocrinol. 46 (2017) 15–31.
[57] M. Huttemann, I. Lee, A. Pecinova, P. Pecina, K. Przyklenk, J.W. Doan, Regulation of oxidative phosphorylation, the mitochondrial membrane potential, and their role in human disease, J. Bioenerg. Biomembr. 40 (2008) 445–456.
[58] C. Ploumi, I. Daskalaki, N. Tavernarakis, Mitochondrial biogenesis and clearance: a balancing act, FEBS J. 284 (2017) 183–195.
[59] H.M. Reichardt, J.P. Tuckermann, M. Gottlicher, M. Vujic, F. Weih, P. Angel, P. Herrlich, G. Schutz, Repression of inflammatory responses in the absence of DNA binding by the glucocorticoid receptor, EMBO J. 20 (2001) 7168–7173.
[60] S. Amar, L. Smith, G.B. Fields, Matrix metalloproteinase collagenolysis in health and disease, Biochim. Biophys. Acta Mol. Cell Res. 1864 (2017) 1940–1951.
[61] T. Endo, T. Kiya, T. Goto, H. Henmi, K. Manase, H. Honnma, T. Baba, S. Ishioka, T. Hayashi, M. Chida, K. Arima, K. Yamazaki, M. Kanaya, A. Azumaguchi, O. Moriwaka, H. Kamiya, T. Saito, Significance of matrix metalloproteinases in the pathophysiology of the ovary and uterus, Reprod. Med. Biol. 5 (2006) 235–243.
[62] P.J. Burton, A.M. Dharmarajan, S. Hisheh, B.J. Waddell, Induction of myometrial 11beta-hydroxysteroid dehydrogenase type 1 messenger ribonucleic acid and protein expression late in rat pregnancy, Endocrinology 137 (1996) 5700–5706.
[63] T. Rhen, S. Grissom, C. Afshari, J.A. Cidlowski, Dexamethasone blocks the rapid biological effects of 17beta-estradiol in the rat uterus without antagonizing its global genomic actions, FASEB J. 17 (2003) 1849–1870.
[64] A.G. Gunin, V.U. Emelianov, A.S. Tolmachev, Expression of estrogen receptor-alpha, glucocorticoid receptor, beta-catenin and glycogen synthase kinase-3beta in the uterus of mice following long-term treatment with estrogen and glucocorticoid hormones, Eur. J. Obstet. Gynecol. Reprod. Biol. 107 (2003) 62–67.
[65] X.D. Yang, D.X. Xiang, Y.Y. Yang, Role of E3 ubiquitin ligases in insulin resistance, Diabetes Obes. Metab. 18 (2016) 747–754.
[66] J.J. Lim, P.D.A. Lima, R. Salehi, D.R. Lee, B.K. Tsang, Regulation of androgen receptor signaling by ubiquitination during folliculogenesis and its possible dysregulation in polycystic ovarian syndrome, Sci. Rep. 7 (2017) 10272.
[67] E.R. Weikum, M.T. Knuesel, E.A. Ortlund, K.R. Yamamoto, Glucocorticoid receptor control of transcription: precision and plasticity via allostery, Nat. Rev. Mol. Cell Biol. 18 (2017) 159–174.
[68] M. Puttabyatappa, V. Padmanabhan, Ovarian and extra-ovarian mediators in the development of polycystic ovary syndrome, J. Mol. Endocrinol. 61 (2018) R161–R184.
[69] P. Elustondo, L.A. Martin, B. Karten, Mitochondrial cholesterol import, Biochim. Biophys. Acta Mol. Cell Biol. Lipids 1862 (2017) 90–101.
[70] Y. Zhao, C. Zhang, Y. Huang, Y. Yu, R. Li, M. Li, N. Liu, P. Liu, J. Qiao, Up-regulated expression of WNT5a increases inflammation and oxidative stress via PI3K/AKT/NF-kappaB signaling in the granulosa cells of PCOS patients, J. Clin. Endocrinol. Metab. 100 (2015) 201–211.
[71] O. Koc, S. Ozdemirici, M. Acet, U. Soyturk, S. Aydin, Nuclear factor-kappaB expression in the endometrium of normal and overweight women with polycystic ovary syndrome, J. Obstet. Gynaecol. 37 (2017) 924–930.
[72] L. Orostica, I. Astorga, F. Plaza-Parrochia, C. Vera, V. Garcia, R. Carvajal, F. Gabler, C. Romero, M. Vega, Proinflammatory environment and role of TNF-alpha in endometrial function of obese women having polycystic ovarian syndrome, Int. J. Obes. 40 (2016) 1715–1722.
[73] H. Henmi, T. Endo, K. Nagasawa, T. Hayashi, M. Chida, N. Akutagawa, M. Iwasaki, Y. Kitajima, T. Kiya, A. Nishikawa, K. Manase, R. Kudo, Lysyl oxidase and MMP-2 expression in dehydroepiandrosterone-induced polycystic ovary in rats, Biol. Reprod. 64 (2001) 157–162.
[74] D.L. Segaloff, H.Y. Wang, J.S. Richards, Hormonal regulation of luteinizing hormone/chorionic gonadotropin receptor mRNA in rat ovarian cells during follicular development and luteinization, Mol. Endocrinol. 4 (1990) 1856–1865.
[75] S. Matthaei, M. Stumvoll, M. Kellerer, H.U. Haring, Pathophysiology and pharmacological treatment of insulin resistance, Endocr. Rev. 21 (2000) 585–618.
[76] P.S. LaPolt, M. Oikawa, X.C. Jia, C. Dargan, A.J. Hsueh, Gonadotropin-induced up- and down-regulation of rat ovarian LH receptor message levels during follicular growth, ovulation and luteinization, Endocrinology 126 (1990) 3277–3279.
[77] H. Peegel, J. Randolph Jr., A.R. Midgley, K.M. Menon, In situ hybridization of luteinizing hormone/human chorionic gonadotropin receptor messenger ribonucleic acid during hormone-induced down-regulation and the subsequent recovery in rat corpus luteum, Endocrinology 135 (1994) 1044–1051.
[78] E.T. Korgun, G. Dohr, G. Desoye, R. Demir, U.A. Kayisli, T. Hahn, Expression of insulin, insulin-like growth factor I and glucocorticoid receptor in rat uterus and embryo during decidualization, implantation and organogenesis, Reproduction 125 (2003) 75–84.
[79] H. Zhang, M. Yi, Y. Zhang, H. Jin, W. Zhang, J. Yang, L. Yan, R. Li, Y. Zhao, J. Qiao, High-fat diets exaggerate endocrine and metabolic phenotypes in a rat model of DHEA-induced PCOS, Reproduction 151 (2016) 431–441.
[80] J. Dupont, R.J. Scaramuzzi, Insulin signalling and glucose transport in the ovary and ovarian function during the ovarian cycle, Biochem. J. 473 (2016) 1483–1501.
[81] M. Noroozzadeh, S. Behboudi-Gandevani, A. Zadeh-Vakili, F. Ramezani Tehrani, Hormone-induced rat model of polycystic ovary syndrome: a systematic review, Life Sci. 191 (2017) 259–272.